

Tail waiting times and the extremes of stochastic processes

James E. Johndrow
Duke University, Durham, NC USA
jj@stat.duke.edu

Robert L. Wolpert
Duke University, Durham, NC USA
wolpert@stat.duke.edu

May 16, 2022

Abstract

In applications where extreme dependence at different spatial locations is of interest, data are almost always time-indexed. When extremes do not occur contemporaneously, existing methods for inference and modeling in this setting often choose window sizes or introduce dependence in parameters with the goal of preserving temporal information. We propose an alternative paradigm for inference on tail dependence in stochastic processes with arbitrary temporal dependence structure in the extremes, based on the idea that the information on strength of tail dependence at different locations and the temporal structure in this dependence are both encoded in waiting times between exceedances of high thresholds at different locations. We construct a class of space/time-indexed stochastic processes with tail dependence obtained by endowing the support points in de Haan’s spectral representation of max-stable processes with velocities and lifetimes. We extend Smith’s model to these max-stable velocity processes and obtain the distribution of waiting times between extreme events at multiple locations. Motivated by this result, a new characterization of tail dependence is proposed that is a function of the distribution of waiting times between threshold exceedances, and an inferential framework is constructed for quantifying the strength of extremal dependence and assessing uncertainty in this paradigm. The method is applied to climatological, financial, and electrophysiology data.

Keywords: extreme value; max-stable process; peaks-over-thresholds; tail dependence; time series; waiting time.

1 Introduction

A *max-stable process* is defined by de Haan [11] as a stochastic process $Y(x)$ on an index set \mathcal{X} with the property that, for all integers $n \in \mathbb{N}$,

$$Y(\cdot) \stackrel{\mathcal{D}}{=} \frac{1}{n} \bigvee_{i=1}^n Y_i(\cdot), \quad (1)$$

where $\{Y_i\}$ are iid copies of Y , where “ \vee ” denotes pointwise maximum, and where for two stochastic processes Y, Z the relation $Z(\cdot) \stackrel{\mathcal{D}}{=} Y(\cdot)$ means that all their finite-dimensional marginal distributions agree. Slightly different definitions appear elsewhere in the literature (33; 7, §9.3; 30; 5, §8.2; 12, §9.2). Some authors use the term “*simple* max-stable process” for those which satisfy (1) (and hence

have Fréchet univariate marginal distributions with shape $\alpha = 1$) and extend the class of max-stable processes to those satisfying

$$Y(\cdot) \stackrel{\mathcal{D}}{=} \left[\bigvee_{i=1}^n Y_i(\cdot) - b_n(\cdot) \right] / a_n(\cdot)$$

for suitable sequences of functions $a_n(\cdot) > 0$, $b_n(\cdot)$. In the spatial or spatio-temporal setting, one usually takes $\mathcal{X} = \mathbb{R}^d$ for some integer d . This model is quite general in the sense that if there exist \mathcal{X} -indexed sequences $a_n(x)$ and $b_n(x)$ and iid processes $w_n(x)$ such that $[\bigvee_{i=1}^n w_i(x) - b_n(x)]/a_n(x)$ converges in distribution then the limit must be a max-stable process [12, Thm 9.2.3] (after transforming to Fréchet marginals, for a simple max-stable process).

In applications where multivariate or spatial extremes are of interest, typically one has a collection of observations $w(\mathbf{x}, t) = (w(x_1, t), \dots, w(x_n, t))$ of a stochastic process $\{W(x, t)\}$ at a collection of locations x_1, \dots, x_n and times t_1, \dots, t_p in some study period $[T_0, T_0 + T]$. These observations could represent hourly precipitation, maximum daily wind speed, or, if we treat the spatial index set \mathcal{X} as a latent coordinate in an abstract attribute space, essentially any multivariate time series, such as daily stock prices.

There are two competing paradigms for statistical inference on max-stable processes based on multivariate time series. The first is the max-over-windows (MoW) approach, which collapses observations $w(\mathbf{x}, t)$ of a space/time-indexed process $\{W(x, t)\}$ to observations that are (approximately) from a max-stable process $Y(x)$ by selecting a time window width $\Delta t > 0$, setting $s_j := T_0 + j\Delta t$, and setting $y_j(\mathbf{x}) := \sup\{w(\mathbf{x}, t) : t \in [s_j, s_{j+1})\}$ [38, 39]. The data $y_j(\mathbf{x}), j = 0, \dots, [T/\Delta t]$ are then used for estimation and inference.

An alternative is the peaks-over-thresholds (PoT) approach [10, 31], which keeps all those observations $w(\mathbf{x}, t)$ that exceed a specified threshold, then treats these observations as realizations of a max-stable process. Various ways of thresholding have been proposed, including: keeping observations at times t for which $\max_{i=1}^n w(x_i, t)$ exceeds a pre-specified threshold [28, 6]; fixing a specific component (say, x_1) and keeping observations at times t where $w(x_1, t)$ exceeds a threshold [20, 19, 9, 1]; and, keeping all observations at times t where some vector norm $\|w(\cdot, t)\|$ exceeds a threshold [8, 2].

Extreme events often cluster temporally: they tend to occur nearby in time, but not necessarily at *identical* times. Temporal structure can be accounted for in the context of both MoW and PoT approaches in a variety of ways. Perhaps the most common way is by choosing the window size in a MoW approach with the goal that dependence across consecutive time windows should be small. Window lengths are often selected based on observed sizes of extreme observation clusters [40, 23]. A common model for temporally dependent spatial extremes that fits broadly into the MoW context is the Multivariate Maximum of Moving Maxima (M4) model [34, 21]. However, MoW methods have the drawback that they tend to discard a larger portion of the data than PoT. Also, artifacts can arise from the arbitrary location of the time window boundaries. Estimation procedures for these models also tend to be complex and multi-stage, resulting in potential loss of efficiency.

Under the PoT approach, some temporal structure must be introduced into the model to accommodate dependency for temporally lagged extremes at different locations [see, e.g., 32, 24, 22, 4, 3]. Without such structure, dependency information is lost for observations of a max-stable process whose threshold exceedances occur at time lags exceeding the sampling rate.

This is illustrated in Figure 1. Extreme values of the variable Y_1 are always followed by extreme values at Y_2 exactly two time units later (Y_2 also has some additional extreme events that occur randomly). Two settings in which this aspect of PoT methods is obviously problematic are when

the exceedance at x_1 *causes* a subsequent exceedance at x_2 ; and when x_1 and x_2 are arranged spatially such that extreme events tend to occur first at x_1 and then later at x_2 , perhaps because the phenomenon causing the exceedances (e.g., a weather event) moves in that direction. While this can be addressed by introducing temporal dependence in parameters, this results in more complex modeling, places more demands on usually limited data, and can complicate selection of an appropriate threshold.

The first main contribution of this work is to propose an alternative paradigm for inference on tail dependence between spatial locations with arbitrary temporal structure. The underlying idea is that waiting times between threshold exceedances at different sites contain information on extremal dependence across both space and time—specifically, that under positive extreme dependence the time lags between thresholds will be *shorter* than under independence. To provide a canonical setting in which to study properties of this approach, we propose a heavy-tailed stochastic process with spatio-temporal dynamics, so that temporal dependence in extreme events can be accommodated naturally. To offer intuition for our proposed model, recall that the process $Z(x) := \sup_j u_j k(x, \xi_j)$ is max-stable [30] if $k : \mathcal{X} \times \mathcal{X} \rightarrow \mathbb{R}_+$ is a nonnegative kernel satisfying $\int_{\mathcal{X}} k(x, \xi) m(d\xi) = 1$ and $\{u_j, \xi_j\}$ are points of a Poisson random Borel measure on $\mathbb{R}_+ \times \mathcal{X}$ with intensity measure proportional to $u^{-2} du m(d\xi)$ for some σ -finite Borel reference measure $m(dx)$ on \mathcal{X} . A single realization from $Z(x)$ for a bivariate Gaussian kernel $k(x, \xi)$ is shown in the right panel of Figure 1. Kernels associated

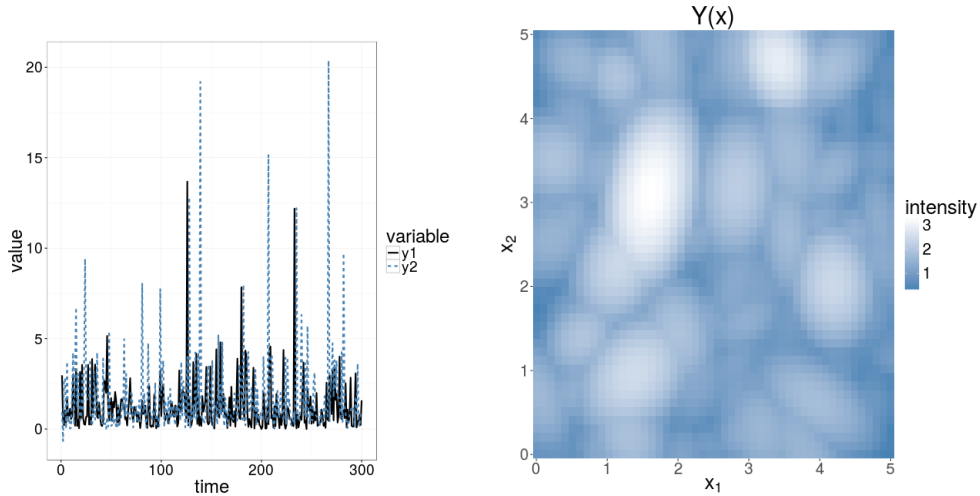


Figure 1: Left panel: example of two time series in which large values of one (Y_1) are followed by large values of the other (Y_2) two time units later. Right panel: a realization of a Gaussian max stable process; blue indicates small values, white large values.

with large values of u_j are clearly discernible. The new stochastic process proposed here endows the points ξ_j with random velocities, birth times, lifetimes, and shapes, making the process dynamic and inducing a temporal dependence structure. As a consequence, time-indexed multivariate data in this paradigm are viewed as a single realization from what we will call a *max-stable velocity process*, rather than multiple (possibly dependent) realizations of a max-stable process. The resulting process can be visualized as a dynamic version of the sample realization in Figure 1 in which the elliptical light regions appear at random times with random orientations and eccentricities, move with random

velocities, and then disappear.

The other main contribution of this work is to propose a method for inference on extreme dependence that does not require modeling the process explicitly. Instead, we model waiting times between thresholds exceedances at pairs of locations, so that inference can be done using only the exceedance time data. Under positive dependence, waiting times between exceedances are systematically shorter than they would be under independence.

We show that the waiting times between exceedances for the max-stable velocity process are distributed as mixtures of exponential distributions and an atom at zero. Further, the waiting time distributions under independence are also mixtures of exponentials and a point mass, but with different rate and mixture parameters. By fitting these two models to data and performing model comparison, we obtain a measure of extreme dependence that naturally captures time lags and exposes differences in the temporal structure of dependence across space. While we focus on inference in the setting where the data are thought to originate from a max-stable velocity process, the use of waiting times to model extreme dependence is general and can be applied in settings where the max-stable velocity process is considered inadequate by choosing a fully nonparametric model for the waiting times.

2 Model

In this section we construct the max-stable velocity process and derive some of its properties, with a focus on the distribution of waiting times between threshold exceedances.

2.1 Max-stable velocity processes

The max-stable velocity process is constructed by extending the spectral characterization of de Haan [11] and its continuous-path extension by Resnick and Roy [27]:

Theorem 2.1 (after de Haan and Resnick and Roy). *Let $\{(u_j, \xi_j)\}_{j \geq 1}$ be the points of a Poisson process on $\mathbb{R}_+ \times \mathbb{R}^d$ with intensity measure proportional to $u^{-2} du d\xi$. Let $\{Y(x)\}_{x \in \mathbb{R}^d}$ be a path-continuous max-stable process with unit Fréchet margins. Then there exist nonnegative continuous functions $\{k(x, \xi) : x, \xi \in \mathbb{R}^d\}$ such that*

$$\int_{\mathbb{R}^d} k(x, \xi) d\xi = 1 \quad \forall x \in \mathbb{R}^d$$

for which

$$\{Y(x)\}_{x \in \mathbb{R}^d} \stackrel{\mathcal{D}}{=} \left\{ \sup_{j \geq 1} u_j k(x, \xi_j) \right\}_{x \in \mathbb{R}^d}, \quad (2)$$

where $\stackrel{\mathcal{D}}{=}$ denotes equality in distribution. Moreover, any process defined by the right side of (2) is max-stable.

A useful heuristic for de Haan's spectral characterization is that of weather extremes: the locations $\{\xi_j\}$ of the support points are taken to be storm centers, the kernel functions $k(x, \xi_j)$ describe the shape of the storm, and the marks $\{u_j\}$ quantify storm severity. In this context, the process realization is the maximum over some period of time of a climatological quantity, such as precipitation or temperature. To create a time-indexed process, we endow the points ξ_j with birth times,

lifetimes, velocities, and shapes. This approach has the advantage of easily extending the physical interpretation of the points ξ_j as storms or, more generally “events.” Now, the storms will move and have finite lifespans.

Specifically: fix positive numbers $\beta > 0$ and $\delta > 0$ and a Borel probability measure $\pi(da)$ on a Polish “attribute space” \mathcal{A} . Define a σ -finite Borel measure

$$\nu(d\omega) := \beta u^{-2} du \, d\xi \, d\sigma \, \delta e^{-\delta\tau} d\tau \, \pi(da) \quad (3)$$

on the space $\Omega := \mathbb{R}_+ \times \mathbb{R}^d \times \mathbb{R} \times \mathbb{R}_+ \times \mathcal{A}$, and let $\mathcal{N}(d\omega) \sim \text{Po}(\nu(d\omega))$ be a Poisson random measure on Ω with intensity $\nu(d\omega)$ — i.e., a measure that assigns independent random variables $\mathcal{N}(B_j) \sim \text{Po}(\nu(B_j))$ to disjoint Borel sets $B_j \subset \Omega$. Fix a nonnegative function $k : \mathbb{R}^d \times \mathbb{R} \times \mathbb{R}^d \times \mathbb{R} \times \mathbb{R}_+ \times \mathcal{A} \rightarrow \mathbb{R}_+$ that satisfies $\int_{\mathbb{R}^d} k(x, \cdot) x, t; \xi, \sigma, \tau, a \, d\xi = 1$ for each x, t, σ, τ, a . Using the climatological heuristic, the support points $\{\omega_j\} = \{(u_j, \xi_j, \sigma_j, \tau_j, a_j)\}$ of $\mathcal{N}(d\omega)$ can be thought of as representing storms of magnitudes $u_j > 0$, initiating at locations $\xi_j \in \mathbb{R}^d$ at times $\sigma_j \in \mathbb{R}$, with lifetimes $\tau_j \in \mathbb{R}_+$ and attribute vectors a_j that may include velocities v_j , shapes Λ_j , or other features. For any location $x \in \mathbb{R}^d$ and time $t \in \mathbb{R}$, define

$$Y(x, t) := \sup_j \{u_j k(x, t; \xi_j, \sigma_j, \tau_j, a_j)\} \quad t \in \mathbb{R} \quad (4a)$$

$$Y^*(x, t) := \sup_{0 \leq s \leq t} Y(x, s), \quad t \geq 0. \quad (4b)$$

We refer to (4a) as a *max-stable velocity (MSV) process* and (4b) as the corresponding *maximal MSV process*.

In the sequel we will take $\mathcal{A} = (\mathbb{R}^d \times \mathcal{P}^d)$ with elements $a_j = (v_j, \Lambda_j) \in \mathcal{A}$ that consist of a velocity vector $v_j \in \mathbb{R}^d$ and a shape matrix $\Lambda_j \in \mathcal{P}^d$, an element of the cone \mathcal{P}^d of positive-definite $d \times d$ matrices. Let $\varphi : \mathbb{R}^d \rightarrow \mathbb{R}_+$ be a continuous pdf satisfying $\int_{\mathbb{R}^d} \varphi(z) dz = 1$ that is non-increasing in $z'z$ and, for $\Lambda \in \mathcal{P}^d$, set $\varphi_\Lambda(z) := |\Lambda|^{1/2} \varphi(\Lambda^{1/2} z)$ (here $|\Lambda|$ denotes the determinant of $\Lambda \in \mathcal{P}^d$). We take k to have the specific form

$$k(x, t; \xi, \sigma, \tau, a) = \varphi_\Lambda(x - \xi - v(t - \sigma)) \mathbf{1}_{\{\sigma \leq t < \sigma + \tau\}}, \quad (5)$$

the magnitude at time t and location $x \in \mathbb{R}^d$ of a storm of unit severity that originated at location $\xi \in \mathbb{R}^d$ at a time $\sigma < t$ and moved at velocity $v \in \mathbb{R}^d$ for time $(t - \sigma)$. We write $Y \sim \text{MSV}(\beta, \delta, \pi, \varphi)$ to denote a process of the form (4a) with k defined by (5) and $\nu(d\omega)$ as in (3). This includes and generalizes the Gaussian and Student t kernels proposed as models for the generic max-stable process by Smith [33].

2.2 Main results

Max-stable velocity processes are in fact space-time indexed forms of the max-stable process, as shown in Theorem 2.2. All proofs are deferred to the Appendix or found in Supplementary Materials.

Theorem 2.2 (Max-stable velocity processes are max-stable). *If $Y \sim \text{MSV}(\beta, \delta, \pi, \varphi)$, then Y is max-stable jointly in (x, t) on the index set $\mathbb{R}^d \times \mathbb{R}_+$.*

Theorem 2.2 is shown by verifying the definition in (1) directly— that is, by verifying that the process is “stable” under finite maxima. It turns out that the maximal MSV process $Y^*(x, t)$ of (4b) is also max-stable.

Theorem 2.3 (Maximal MSV process is max-stable). *If $Y \sim \text{MSV}(\beta, \delta, \pi, \varphi)$, then $Y^*(x, t)$ is max-stable in (x, t) on the index set $\mathbb{R}^d \times \mathbb{R}_+$.*

Therefore, if data are generated from a MSV process and transformed by taking blockwise maxima, the transformed data are realizations of a max-stable process. This result provides a link between traditional methods and the alternative we propose.

In addition to the marginal and joint distribution of the max-stable velocity process, we are also interested in the distribution of *waiting times* between threshold exceedances at distinct points, as these will eventually form the basis for inference. For two arbitrary locations $x_1, x_2 \in \mathbb{R}^d$ and threshold levels $y_1, y_2 \in \mathbb{R}_+$, define the random variables

$$\kappa_i := \inf_{t \geq 0} \{t : Y(x_i, t) > y_i\}, \quad i = 1, 2$$

Then $\kappa_\Delta := |\kappa_1 - \kappa_2|$ is the waiting time between first exceedances of levels y_1 at x_1 and of y_2 at x_2 , in either order. Theorem 2.4 gives the marginal distribution of the max-stable velocity process $Y(x, t)$ and that of the waiting times κ_i until first exceedance.

Theorem 2.4 (Marginals and waiting times). *The max-stable velocity process has unit Fréchet marginals, with distribution function $P[Y(x, t) \leq y] = e^{-\beta/\delta y}$ for $y > 0$. The marginal waiting time distribution is given for $t \geq 0$ by*

$$P[\kappa_i > t] = \exp \left(-\frac{\beta}{\delta y_i} - t \frac{\beta}{\delta y_i} \left\{ \delta + \int_{\mathbb{R}^d \times \mathcal{P}^d \times v^\perp} \varphi_\Lambda(\zeta) d\zeta |v| \pi(dv d\Lambda) \right\} \right), \quad (6)$$

where $v^\perp := \{\zeta \in \mathbb{R}^d : v' \Lambda \zeta = 0\}$ denotes the orthogonal complement of the span of v in the Λ metric. This is a mixture of a point-mass at zero with weight $1 - \exp(\beta/\delta y_i)$ and an exponential distribution with a shape-dependent rate constant that increases monotonically in the mean particle speed.

Corollary 2.5 (Distribution of Y^*). *The distribution of $Y^*(x_i, t) = P[Y^*(x_i, t) < y_i]$ is given by (6).*

Thus the waiting time distribution and the distribution of $Y^*(x, t)$, unlike the marginal distribution of $Y(x, t)$, depends on velocity and shape. For Gaussian kernels φ , (6) has a simple expression:

Corollary 2.6 (Waiting time distribution for Gaussian kernels). *For Gaussian kernels $\varphi(z) = (2\pi)^{-d/2} \exp(-z'z/2)$,*

$$P[\kappa_i > t] = \exp \left(-\frac{\beta}{\delta y_i} - t \frac{\beta}{\delta y_i} \left\{ \delta + E_\pi \left[(v' \Lambda v / 2\pi)^{\frac{1}{2}} \right] \right\} \right). \quad (7)$$

Thus in the Gaussian case, the marginal waiting times converge to zero in distribution as $E_\pi[\sqrt{v' \Lambda v}] \rightarrow \infty$. Theorem 2.7 gives the joint distribution of the max-stable velocity process at finite collections of locations $\{x_i\}_{1 \leq i \leq n}$ and times $\{t_i\}_{1 \leq i \leq n}$.

Theorem 2.7 (Joint CDF). *Let $Y \sim \text{MSV}(\beta, \delta, \pi, \varphi)$ be a max-stable velocity process and let $\{x_i\}_{1 \leq i \leq n} \subset \mathbb{R}^d$ and $\{t_i\}_{1 \leq i \leq n} \subset \mathbb{R}$ for some integer $n \in \mathbb{N}$. The joint CDF for $\{Y(x_i, t_i)\}_{1 \leq i \leq n}$ is given by*

$$F(y_1, \dots, y_n) := P\left(\cap_{1 \leq i \leq n} [Y(x_i, t_i) \leq y_i]\right) = \exp\left(-\nu(\cup_{1 \leq i \leq n} B_i)\right) \quad (8a)$$

for $B_i := \{\omega : Y(x_i, t_i) > y_i\}$, with

$$\nu(\cup_{1 \leq i \leq n} B_i) = \sum_{1 \leq i \leq n} \nu(B_i) - \sum_{i \neq j} \nu(B_i \cap B_j) + \sum_{i \neq j \neq k} \nu(B_i \cap B_j \cap B_k) - \dots, \quad (8b)$$

the alternating sum of terms

$$\nu(\cap_{i \in J} B_i) = \frac{\beta}{\delta} e^{-\delta(t^J - t_J)} \int_{\mathbb{R}^d \times \mathcal{A}} \min_{j \in J} \left\{ \frac{\varphi_\Lambda(x_j - vt_j - z)}{y_j} \right\} dz \pi(dv d\Lambda) \quad (8c)$$

for subsets $J \subseteq \{1, \dots, n\}$. Here $t^J := \max\{t_j\}$ denotes the maximum and $t_J := \min\{t_j\}$ the minimum of $\{t_j\}_{j \in J}$.

While the univariate marginal distributions of $Y(x, t)$ do not depend on $\pi(dv d\Lambda)$ at all, higher order marginal distributions do. For example,

Corollary 2.8 (Gaussian MSV process joint CDF at two points). *For the Gaussian max-stable velocity process with $\varphi(z) = (2\pi)^{-d/2} \exp(-z'z/2)$, the bivariate distribution is given by $F(y_1, y_2) = \exp(-\nu(B_1 \cup B_2))$ with*

$$\begin{aligned} \nu(B_1 \cup B_2) &= \frac{\beta}{\delta} (1 - e^{-\delta|t_2 - t_1|}) \left(\frac{1}{y_1} + \frac{1}{y_2} \right) + \frac{\beta}{\delta} e^{-\delta|t_2 - t_1|} \\ &\times \int_{\mathcal{P}^d \times \mathbb{R}^d} \left\{ \frac{1}{y_1} \Phi\left(\frac{S_\Lambda(v)}{2} - \frac{\log(y_1/y_2)}{S_\Lambda(v)}\right) + \frac{1}{y_2} \Phi\left(\frac{S_\Lambda(v)}{2} - \frac{\log(y_2/y_1)}{S_\Lambda(v)}\right) \right\} \pi(dv d\Lambda) \end{aligned} \quad (9)$$

where $\Phi(\cdot)$ is the standard Gaussian CDF and $S_\Lambda(v) := \sqrt{\Delta'_v \Lambda \Delta_v}$ for $\Delta_v := (x_2 - x_1) - (t_2 - t_1)v$.

Equation (9) generalizes Smith [33, equation 3.1], and reduces to it if $t_1 = t_2$ and if π is a unit point mass. It leads to an explicit expression for the likelihood function for the Gaussian max-stable velocity process with observations at two locations and times. This expression could be used to fit the max-stable velocity process to data by maximum composite likelihood.

Theorem 2.9 gives an expression for the waiting times between first exceedances under independence, which provides a null distribution in the approach to inference proposed in Section 3.

Theorem 2.9 (Waiting times between exceedances under independence). *Suppose that κ_1 and κ_2 are independent, each with the distribution given in (6) of Theorem 2.4. Then the distribution of κ_Δ is given for $t \geq 0$ by*

$$\begin{aligned} \mathbb{P}[\kappa_\Delta > t] &= (1 - e^{-a_2})e^{-a_1 - b_1 t} + (1 - e^{-a_1})e^{-a_2 - b_2 t} \\ &+ \frac{b_2 e^{-a_1 - a_2}}{b_1 + b_2} e^{-b_1 t} + \frac{b_1 e^{-a_1 - a_2}}{b_1 + b_2} e^{-b_2 t} \\ &= \left\{ \frac{b_1 e^{-a_1 - a_2}}{b_1 + b_2} + \frac{(1 - e^{-a_2})}{e^{a_1}} \right\} e^{-b_1 t} + \left\{ \frac{b_2 e^{-a_1 - a_2}}{b_1 + b_2} + \frac{1 - e^{-a_1}}{e^{a_2}} \right\} e^{-b_2 t} \end{aligned} \quad (10)$$

where

$$a_i = \frac{\beta}{\delta y_i} \quad b_i = \frac{\beta}{\delta y_i} \left\{ \delta + \int_{\mathbb{R}^d \times \mathcal{P}^d \times v^\perp} \varphi_\Lambda(\zeta) d\zeta |v| \pi(dv d\Lambda) \right\}.$$

Thus, when $\kappa_1 \perp \kappa_2$, κ_Δ is distributed as a mixture with three components: a point mass at zero and two exponential distributions with rates b_1 and b_2 . For the Gaussian kernel, the integral expression over $\mathcal{P}^d \times \mathbb{R}^d \times v^\perp$ is given by $\mathbb{E}_\pi \left[(v' \Lambda v / 2\pi)^{\frac{1}{2}} \right]$.

Theorem 2.10 gives the distribution of κ_Δ in the special case of $v = 0$. This result is useful in understanding the effect of velocity on the waiting time distribution in the general case.

Theorem 2.10 (waiting times between exceedances when $v \equiv 0$). *Suppose $\pi(\{0\} \times \mathcal{P}^d) = 1$ in the Gaussian max-stable velocity model, so $v \equiv 0$ almost surely. Then the distribution of κ_Δ is given for $t \geq 0$ by*

$$\mathbb{P}[\kappa_\Delta = 0] = 1 - e^{-\lambda_0}(e^{-\lambda_1} + e^{-\lambda_2}) + e^{-\lambda_+}(1 + \frac{\lambda_0}{\lambda_+}) \quad (11a)$$

$$\begin{aligned} \mathbb{P}[\kappa_\Delta > t] &= e^{-(\lambda_0 + \lambda_2)(1 + \delta t)} \left[1 - \frac{\lambda_0 + \lambda_2}{\lambda_+} e^{-\lambda_1} \right] \\ &\quad + e^{-(\lambda_0 + \lambda_1)(1 + \delta t)} \left[1 - \frac{\lambda_0 + \lambda_1}{\lambda_+} e^{-\lambda_2} \right] \end{aligned} \quad (11b)$$

a mixture of an atom at zero and two exponential distributions with rates λ_1, λ_2 . The quantities $\{\lambda_j\} \subset \mathbb{R}_+$ are given by $\lambda_+ := \lambda_0 + \lambda_1 + \lambda_2$ and, for $j = 0, 1, 2$,

$$\begin{aligned} \lambda_0 &= \frac{\beta}{\delta} \int_{\mathbb{R}^d \times \mathcal{A}} \left[\frac{1}{y_1} \mathbf{1}_{\{\frac{\varphi_\Lambda(z)}{\varphi_\Lambda(z + \Delta_0)} < \frac{y_1}{y_2}\}} + \frac{1}{y_2} \mathbf{1}_{\{\frac{\varphi_\Lambda(z)}{\varphi_\Lambda(z - \Delta_0)} < \frac{y_2}{y_1}\}} \right] \varphi_\Lambda(z) dz \pi(da) \\ \lambda_1 &= \frac{\beta}{\delta} \int_{\mathbb{R}^d \times \mathcal{A}} \left[\frac{1}{y_1} \mathbf{1}_{\{\frac{\varphi_\Lambda(z + \Delta_0)}{\varphi_\Lambda(z)} < \frac{y_2}{y_1}\}} - \frac{1}{y_2} \mathbf{1}_{\{\frac{\varphi_\Lambda(z)}{\varphi_\Lambda(z - \Delta_0)} < \frac{y_2}{y_1}\}} \right] \varphi_\Lambda(z) dz \pi(da) \\ \lambda_2 &= \frac{\beta}{\delta} \int_{\mathbb{R}^d \times \mathcal{A}} \left[\frac{1}{y_2} \mathbf{1}_{\{\frac{\varphi_\Lambda(z - \Delta_0)}{\varphi_\Lambda(z)} < \frac{y_1}{y_2}\}} - \frac{1}{y_1} \mathbf{1}_{\{\frac{\varphi_\Lambda(z)}{\varphi_\Lambda(z + \Delta_0)} < \frac{y_1}{y_2}\}} \right] \varphi_\Lambda(z) dz \pi(da) \\ \lambda_+ &= \frac{\beta}{\delta} \int_{\mathbb{R}^d \times \mathcal{A}} \left[\frac{1}{y_1} \mathbf{1}_{\{\frac{\varphi_\Lambda(z)}{\varphi_\Lambda(z + \Delta_0)} < \frac{y_1}{y_2}\}} + \frac{1}{y_2} \mathbf{1}_{\{\frac{\varphi_\Lambda(z)}{\varphi_\Lambda(z - \Delta_0)} > \frac{y_2}{y_1}\}} \right] \varphi_\Lambda(z) dz \pi(da). \end{aligned}$$

with $\Delta_0 := (x_2 - x_1)$ as in Theorem 2.7. The rates are available in closed form for the Gaussian kernel:

$$\begin{aligned} \lambda_0 &= \frac{\beta}{\delta} \int_{\mathcal{A}} \left\{ \frac{1}{y_1} \Phi\left(\frac{1}{S_\Lambda} \log \frac{y_1}{y_2} - \frac{S_\Lambda}{2}\right) + \frac{1}{y_2} \Phi\left(\frac{1}{S_\Lambda} \log \frac{y_2}{y_1} - \frac{S_\Lambda}{2}\right) \right\} \pi(da) \\ \lambda_1 &= \frac{\beta}{\delta} \int_{\mathcal{A}} \left\{ \frac{1}{y_1} \Phi\left(\frac{1}{S_\Lambda} \log \frac{y_2}{y_1} + \frac{S_\Lambda}{2}\right) - \frac{1}{y_2} \Phi\left(\frac{1}{S_\Lambda} \log \frac{y_2}{y_1} - \frac{S_\Lambda}{2}\right) \right\} \pi(da) \\ \lambda_2 &= \frac{\beta}{\delta} \int_{\mathcal{A}} \left\{ \frac{1}{y_2} \Phi\left(\frac{1}{S_\Lambda} \log \frac{y_1}{y_2} + \frac{S_\Lambda}{2}\right) - \frac{1}{y_1} \Phi\left(\frac{1}{S_\Lambda} \log \frac{y_1}{y_2} - \frac{S_\Lambda}{2}\right) \right\} \pi(da) \\ \lambda_+ &= \frac{\beta}{\delta} \int_{\mathcal{A}} \left\{ \frac{1}{y_1} \Phi\left(\frac{1}{S_\Lambda} \log \frac{y_2}{y_1} + \frac{S_\Lambda}{2}\right) + \frac{1}{y_2} \Phi\left(\frac{1}{S_\Lambda} \log \frac{y_1}{y_2} + \frac{S_\Lambda}{2}\right) \right\} \pi(da) \end{aligned}$$

and simplify considerably if $y_1 = y_2$ (see Supplementary Materials).

The next result gives a stochastic bound on the distribution of κ_Δ in the general case. The result is given here for the Gaussian kernel; expressions for the general case can be found in the Appendix.

Theorem 2.11 (Stochastic bound for survival function with nonzero velocity). *Suppose $Y \sim \text{MSV}(\beta, \delta, \pi, \varphi)$ is a Gaussian max-stable velocity process. Then for any two points x_1, x_2 and thresholds y_1, y_2 , κ_Δ satisfies the stochastic ordering*

$$\mathbb{P}[\kappa_\Delta > t] \leq \exp\{-\eta(A)\},$$

with

$$\begin{aligned} \eta(A) = \frac{\beta}{\sqrt{2\pi}} \int_{\mathbb{R}^d \times \mathcal{P}^d} (t - \Delta_{12}) e^{-\delta \Delta_{12}} \left\{ \frac{1}{y_1} \Phi \left(-\frac{S_{\Lambda}^{\perp}(v)}{2} + \frac{\log(y_1/y_2)}{S_{\Lambda}^{\perp}(v)} \right) \right. \\ \left. + \frac{1}{y_2} \Phi \left(-\frac{S_{\Lambda}^{\perp}(v)}{2} - \frac{\log(y_1/y_2)}{S_{\Lambda}^{\perp}(v)} \right) \right\} \sqrt{v' \Lambda v} \pi(d\Lambda dv), \end{aligned} \quad (13)$$

where $S_{\Lambda}^{\perp}(v) := \{(x_2 - x_1)' \Lambda (x_2 - x_1)^{\perp}\}^{1/2}$, $\Delta_{12} := v' \Lambda (x_2 - x_1) / v' \Lambda v$, and $(x_2 - x_1)^{\perp} := (x_2 - x_1) - \Delta_{12} v$ is the projection of $(x_2 - x_1)$ into the orthogonal complement of v in the Λ metric.

Theorem 2.11 shows that for the Gaussian MSV process, κ_{Δ} converges to zero in probability if

$$\mathbb{E}_{\pi} \left[\sqrt{v' \Lambda v} \Phi \left(-\sqrt{(x_2 - x_1)' \Lambda (x_2 - x_1)^{\perp}} \right) \right] \rightarrow \infty.$$

This condition is only slightly stronger than the condition $\mathbb{E}_{\pi}[\sqrt{v' \Lambda v}] \rightarrow \infty$, which is sufficient for the marginal waiting times to converge to zero in probability based on (7). Informally, the difference between these conditions is that $\pi(dv d\Lambda)$ cannot place too much mass on Λ with large eigenvalues, which corresponds to extremely concentrated kernels. This is intuitive: it is difficult for the same point to cause an exceedance at two different locations when the kernels are extremely concentrated, since the volumes of space where exceedances can occur are very small.

It is instructive to compare the result in Theorems 2.10 and 2.11. When $v \equiv 0$, all exceedances occur at birth times or at time zero, so points $\omega \in \Omega$ leading to exceedance when $\pi(\{0\} \times \mathcal{P}^d) = 1$ will also lead to exceedance for any other velocity distribution. Therefore, (11) also provides a stochastic bound on the survival function with nonzero velocity. Taken together, these results imply that expected waiting times decrease as mean speed increases, and the distribution of κ_{Δ} is dominated by a mixture of an atom at zero and exponential distributions. Thus, such mixtures provide a useful model for κ_{Δ} with arbitrary $\pi(dv d\Lambda)$, and the model space of finite mixtures of exponentials with an atom at zero contains the distribution of κ_{Δ} in the max-stable velocity model.

3 Inference: Tail waiting times

Waiting times between exceedances in the max-stable velocity process are given by simple mixtures of exponential distributions and a point mass at zero. Thus, we propose to use the waiting times between exceedances as data to perform inference on tail dependence, bypassing pseudo-likelihood procedures. In this section we propose a novel quantification of tail dependence based on waiting times. We then propose a Bayesian approach to inference for this quantity.

3.1 Waiting times as a measure of extremal dependence

Classically, the tail dependence index of a stochastic process $Y(x)$ at points x_1, x_2 is defined as the limit $\gamma := \lim_{y \rightarrow \infty} \mathbb{P}[Y(x_1) > y \mid Y(x_2) > y]$ of the conditional survival probability. A conceptually similar approach is possible for *tail waiting times* κ_{Δ} . Fix $x_1, x_2 \in \mathbb{R}^d$ and let $\{\mu_{\Delta}\}$ be the family of Borel probability measures on \mathbb{R} induced by the collection of random variables κ_{Δ} , indexed by pairs $(y_1, y_2) \in \mathbb{R}_+^2$, so that for any Borel set A and any (y_1, y_2) we have $\mu_{\Delta}(A; y_1, y_2) = \mathbb{P}[\kappa_{\Delta} \in A]$. We suppress dependence on (y_1, y_2) to simplify notation. Similarly, let μ_{Δ}^{\perp} be the measure induced by

κ_Δ under the assumption $\kappa_1 \perp\!\!\!\perp \kappa_2$, the product measure of the marginal distributions of κ_1 and κ_2 . For any metric $d(\cdot, \cdot)$ on the space of probability measures, define a tail dependence index γ_d based on tail waiting times by

$$\gamma_d := d(\mu_\Delta, \mu_\Delta^\perp), \quad \gamma_d^\infty := \lim_{y_1, y_2 \rightarrow \infty} \gamma_d. \quad (14)$$

In this framework, a value of $\gamma_d^\infty = 0$ corresponds to convergence (in the topology induced by d) as $y_1, y_2 \rightarrow \infty$ of the distribution of κ_Δ to its distribution under independence, while $\gamma_d^\infty > 0$ indicates a discrepancy between the measures that persists asymptotically.

Inference on γ_d requires specification of a metric $d(\cdot, \cdot)$ on probability measures, which we now construct. Let $(\mathbb{H}, \langle \cdot, \cdot \rangle_\mathbb{H})$ be a reproducing kernel Hilbert space on \mathbb{R} with reproducing kernel $\mathcal{K} : \mathbb{R} \times \mathbb{R} \rightarrow \mathbb{R}$ and unit ball $\mathbb{H}_1 := \{f \in \mathbb{H} : \langle f, f \rangle_\mathbb{H} \leq 1\}$. For each $\theta \in \mathbb{R}$ denote by $\mathcal{K}_\theta \in \mathbb{H}$ the function $\mathcal{K}(\theta, \cdot)$, that satisfies $\langle \mathcal{K}_\theta, h \rangle_\mathbb{H} = h(\theta)$ for all $h \in \mathbb{H}$.

The set $\mathcal{P}_\mathcal{K} := \{\text{Borel probability measures } \mu \text{ on } \mathbb{R} \text{ s.t. } \int_\mathbb{R} \sqrt{\mathcal{K}(\theta, \theta)} \mu(d\theta) < \infty\}$ can be embedded into \mathcal{H} by the mapping $\mu \mapsto \mu^\mathbb{H} := \int_\mathbb{R} \mathcal{K}_\theta \mu(d\theta)$. This induces a pseudo-metric on $\mathcal{P}_\mathcal{K}$ by

$$d_\mathcal{K}(\mu_1, \mu_2) := \|\mu_1^\mathbb{H} - \mu_2^\mathbb{H}\|_\mathbb{H} = \sup_{h \in \mathbb{H}_1} \left| \int_\mathbb{R} h(\theta)(\mu_1 - \mu_2)(d\theta) \right| \quad (15)$$

[17, §2.3]. For *characteristic* kernels, including strictly positive-definite ones like the Gaussian kernel we use $\mathcal{K}_G(\theta, \theta') := \exp(-|\theta - \theta'|^2)$, (15) is in fact a metric (i.e., satisfies $d_\mathcal{K}(\mu_1, \mu_2) = 0$ if and only if $\mu_1 = \mu_2$)—a simple consequence of Bochner’s and Plancherel’s Theorems for strictly positive-definite kernels [25, §2.3]. It is this metric we use as “ $d(\cdot, \cdot)$ ” in (14).

This family of metrics has been studied extensively in the literature [16, 35, 36, 37, 17, 25], and an estimator based on empirical measures is given by Minsker et al. [25, Equation (2.12)]. This estimator is both computationally tractable and robust for small samples and high dimensions, motivating our use of it.

Moreover, conditions similar to those required for convergence of the posterior in the Hellinger metric [see 15] imply convergence in $d_\mathcal{K}$, at the same rate [25]. For simplicity, in the sequel we refer to $d_\mathcal{K}$ as the “RKHS distance,” and all of the estimates presented utilize the Gaussian kernel $\mathcal{K}(\theta, \theta') = \exp(-|\theta - \theta'|^2)$.

One alternative to the RKHS metric $d_\mathcal{K}$ is the total variation distance (TV), given by $\|\mu_1 - \mu_2\|_{\text{TV}} := \sup_A |\mu_1(A) - \mu_2(A)|$, where the supremum is taken over Borel sets $A \subset \mathbb{R}$. For one dimensional distributions, a point estimate of $\|\mu_1 - \mu_2\|_{\text{TV}}$ is provided by the Kolmogorov-Smirnov statistic. Another alternative is the Wasserstein W_1 metric, to which $d_\mathcal{K}$ bears some relation.

3.2 Estimating waiting times from observed data

Consider heavy-tailed data $w(\mathbf{x}, t)$ which feature (possibly after transformation) unit Fréchet marginals. For each finite set $\{x_i\} \subset \mathbb{R}^d : i = 1, \dots, n$ of locations, select thresholds $\{y_i\} \subset \mathbb{R}_+$ corresponding to high quantiles of the Fréchet distribution. Compute the marginal waiting times $\{\kappa_i\}$ until first exceedance using Algorithm 1.

The subtraction of $(t_{l+1} - t_l) + (t_f - t_{f-1})$ from $(t_f - t_l)$ in Algorithm 1 is a convention that is easiest to explain by example. Suppose data are observed at three consecutive time points t_{j-2}, t_{j-1}, t_j , and that $w(x_i, t_{j-2}) > y_i, w(x_i, t_j) > y_i$ but $w(x_i, t_{j-1}) \leq y_i$. We cannot know for $\epsilon < \min(t_{j-1} - t_{j-2}, t_j - t_{j-1})$ whether the value of $w(x_i, t_{j-1} \pm \epsilon) > y_i$ or not. Therefore, the waiting time between first exceedances could be arbitrarily close to zero, or as long as $t_j - t_{j-2}$. Subtraction

Data: times t_1, \dots, t_m , data $w(x_i, t_j)$ for $j \leq m$, threshold y_i
Result: Waiting times κ_i until first exceedances of y_i at location x_i
 $F = \{j : 1 < j \leq m, w(x_i, t_j) > y_i, w(x_i, t_{j-1}) \leq y_i\}$; $F = \text{sort}(F, \text{increasing})$;
 $L = \{j : 1 < j \leq m, w(x_i, t_j) \leq y_i, w(x_i, t_{j-1}) > y_i\}$; $L = \text{sort}(L, \text{increasing})$;
if $\min F \leq \min L$ **then**
 | $F = F_{2:|F|}$;
end
if $\max L \geq \max F$ **then**
 | $L = L_{1:(|L|-1)}$;
end
 $N = |F|$; κ = vector of length N ;
for $n = 1, \dots, N$ **do**
 | $f = F_n$; $l = L_n$;
 | $\kappa_n = (t_f - t_l) - ((t_{l+1} - t_l) + (t_f - t_{f-1}))$;
end
return $\kappa_i = \kappa$;
Algorithm 1: Computation of marginal waiting times between first exceedances

of $(t_{l+1} - t_l) + (t_f - t_{f-1})$ results in an observed value of zero. In our approach to inference, we appropriately adjust for the induced bias by imputing observed waiting times. Algorithm 2 returns observed waiting times between first exceedances at pairs of sites $(x_i, x_{i'})$.

Data: times $T_i, T_{i'}$, data $w(x_i, t)$ for $t \in T_i$, $w(x_{i'}, t)$ for $t \in T_{i'}$, thresholds $y_i, y_{i'}$
Result: Waiting times κ_Δ between first exceedances of y_i at location x_i and $y_{i'}$ at location $x_{i'}$
 $F_i = \{t \in T_i : w(x_i, t) > y_i, w(x_i, \max_s \{s \in T_i, s < t\}) \leq y_i\}$; $F_i = \text{sort}(F_i, \text{increasing})$;
 $F_{i'} = \{t \in T_{i'} : w(x_{i'}, t) > y_{i'}, w(x_{i'}, \max_s \{s \in T_{i'}, s < t\}) \leq y_{i'}\}$;
 $N = |F_i|$; κ = vector of length N ;
for $n = 1, \dots, N$ **do**
 | $t = F_{i,n}$; $\Delta = \min_{t_{i'} \in F_{i'}} |t - t_{i'}|$;
 | $\kappa_n = \Delta$;
end
return $\kappa_\Delta = \kappa$;
Algorithm 2: Computation of waiting times between first exceedances at two locations

The resulting data are n vectors κ_i of marginal waiting times until first exceedances and $n(n-1)/2$ vectors of waiting times κ_Δ between first exceedances at pairs of locations $(x_i, x_{i'})$. Clearly, the larger y_i , the fewer observations of first exceedances exist. The effect of the threshold on sample size and the necessity of choosing y_i large enough that values exceeding this threshold have approximately a limiting max-stable velocity distribution are the two opposing considerations in choosing a threshold. Our goal here is mainly to illustrate the potential of the method, so we take the simple approach of choosing thresholds such that there are at least 100 observations of κ_i for each i .

3.3 Estimation of γ_d

We take a model-based approach to estimating μ_Δ and μ_Δ^\perp , guided by Theorems 2.9 and 2.11. If the data originate from a max-stable velocity process, then the marginal waiting time distribution is the mixture of an atom at zero and an exponential distribution given by Theorem 2.4, and the distribution of waiting times between exceedances is stochastically dominated by the expressions in Theorems 2.10 and 2.11. As such, we model κ_i and κ_Δ using a mixture of several exponential components and an atom

$$\kappa \sim \eta_0 \delta_0 + \sum_{j=1}^{K-1} \eta_j \text{Exponential}(\lambda_j). \quad (16)$$

We take a Bayesian approach to inference in this model by specifying the prior distributions $\eta \sim \text{Dirichlet}(1/K, \dots, 1/K)$, and $\lambda_j \sim \text{Gamma}(1, 1)$, and write $\psi = (\eta, \lambda)$ to represent the model parameters. Computation is via a straightforward Gibbs sampler, described in Supplementary Materials. All of the empirical results in the sequel were obtained using $K = 11$ components, and point estimates always correspond to the ergodic average from sample paths obtained from the Gibbs sampler.

The motivation for a Bayesian approach is threefold. First, censoring of κ is common in applications because data are sampled at discrete intervals. This is easy to handle in a Bayesian model by imputing uncensored waiting times. Second, by setting K to be relatively large, the posterior is consistent for the true number of mixture components, and the extraneous components tend to empty [29]. Thus, the Bayesian approach provides an easy way to estimate the number of mixture components and assess model fit. Finally, a Bayesian approach provides estimates of uncertainty in μ_Δ and μ_Δ^\perp without the use of additional procedures.

Estimating models of the form in (16) by MCMC yields approximate posterior samples $\{\psi_i\}$ from $\pi(\psi_i \mid \kappa_i)$ for $i = 1, \dots, n$ and $\{\psi_\Delta\}$ from $\pi(\psi_\Delta \mid \kappa_\Delta)$ for each pair of sites $(i, i') \in \{1, \dots, n\}^2$. To obtain approximate samples from the posterior distribution

$$\pi(\gamma_d \mid \kappa) = \pi(\gamma_d \mid \kappa_i, \kappa_{i'}, \kappa_\Delta), \quad (17)$$

for any pair of sites, follow the procedure:

- (1) For each sampled value of $\{\psi_i, \psi_{i'}\}$, take M samples from the posterior predictive distribution $\pi(\kappa_\Delta^\perp \mid \psi_i, \psi_{i'})$, e.g., by taking M independent samples from the posterior predictive distributions $\pi(\kappa_i \mid \psi_i)$ and $\pi(\kappa_{i'} \mid \psi_{i'})$ and computing $\kappa_\Delta^\perp = |\kappa_i - \kappa_{i'}|$ for each sampled value.
- (2) For each sampled value of ψ_Δ , take M samples from the posterior predictive distribution $\pi(\kappa_\Delta \mid \psi_\Delta)$.
- (3) Compute an estimate of $\gamma_d = d(\mu_\Delta, \mu_\Delta^\perp)$ based on the M samples taken in the previous two steps.
- (4) Repeat (1)–(3) for each retained sample of $\{\psi_i, \psi_{i'}, \psi_\Delta\}$.

The resulting samples are approximately samples from (17). All point estimates $\hat{\gamma}_d$ in the empirical results were obtained from ergodic averages of γ_d .

3.4 Posterior Inference

We now suggest an approach for characterizing the strength of tail dependence given the posterior distribution in (17). For any ψ , let $\kappa_\Delta(\psi)$ be a random variable with distribution given by (16), and let $\mu_\Delta(\psi)$ be the measure induced by $\kappa_\Delta(\psi)$. Consider the random variable d^* given by $d^* := d(\mu_\Delta(\psi_1), \mu_\Delta(\psi_2))$, where $\psi_1, \psi_2 \stackrel{\text{ind}}{\sim} \pi(\psi \mid \kappa_\Delta)$. The distribution of d^* is the posterior distribution of distances between measures induced by the likelihood in (16), and reflects uncertainty about the parameters ψ after having observed the waiting times κ_Δ . If there is strong tail dependence between sites x_i and $x_{i'}$, we would expect $\hat{\gamma}_d$ to be large relative to d^* . Thus, as a basic measure of the relative magnitude of γ_d , we estimate

$$p_d = \mathbb{P}[\gamma_d > d^* \mid \kappa] = \mathbb{E}_{\pi(\gamma_d \mid \kappa) \times \pi(d^* \mid \kappa_\Delta)} \left[\mathbf{1}_{\{d^* < \gamma_d(\mu_\Delta, \mu_\Delta)\}} \right];$$

if p_d is near 1, there is strong evidence for tail dependence.

4 Simulation

In this section, a simulation study is constructed to illustrate the method. The simulation is motivated by extreme weather events, where basic scientific knowledge allows informative choices. Data are simulated from a Gaussian max-stable velocity process with attribute distribution

$$\begin{aligned} \pi(da) = \pi(dr d\phi d\Lambda) &\propto |\Lambda|^{(\nu-k-1)/2} e^{-\text{tr}(\Psi^{-1}\Lambda)/2} r^{-3/2} e^{-(a(r-m)^2)/(2m^2r)} \\ &\times \prod_{h=1}^{k-1} \left[\frac{1}{2} q e^{-q\phi_h} \mathbf{1}_{\{\phi_h > 0\}} + \frac{1}{2} q e^{-q\phi_h} \mathbf{1}_{\{\phi_h < 0\}} \right] dr d\phi d\Lambda, \end{aligned}$$

where $(r, \phi_1, \dots, \phi_{k-1})$ is the polar parametrization of the velocity v . This corresponds to a Wishart distribution for Λ with degrees of freedom ν and shape Ψ , an inverse Gaussian distribution for the magnitude of the velocity r with parameters m, a , and wrapped Laplace distributions with parameter q for the angles $(\phi_1, \dots, \phi_{k-1})$ defining the direction of the velocity in \mathbb{R}^k . The storm lifetimes $\tau \sim \text{Exponential}(\delta)$ and the support points ξ follow a homogeneous spatial Poisson process with rate $\beta d\xi$. The intensity measure in the specification of the process $u \propto u^{-2}$ is improper. For the simulation, we put $u \sim \text{Pareto}(u_{\min}, 1)$, the conditional distribution of u given $u > u_{\min}$. Hyperparameters for the simulation are shown in Table 1.

Table 1: Hyperparameter choices for simulations

	β	u_{\min}	δ	Ψ	ν	m	a	q
value	1/600	1	1/120	I_2	7	1/10	1/2	1/2

The data are simulated on a 10×10 box B . In order to inform hyperparameter choices, this box is taken to roughly represent a 5 000km² area containing the continental United States and southern Canada. As a result, the distributions of velocity and lifetimes of storms are chosen to approximate the behavior of weather events in this geographic region. To set the time scale and allow easier interpretation of results, one unit of time in the simulation is considered one hour. Support points of the marginal process $\mathcal{N}(d\xi d\sigma)$ are sampled on $B \times [0, T]$, with $T = 50 \times 365 \times 24 = 438\,000$, so that the number of support points of $\mathcal{N}(d\xi d\sigma)$ are Poisson distributed with mean $\beta \times T \times 100$. The

choice of $\beta = 1/600$ gives an average of four storms a day forming in the region. Storm lifetimes τ_j are sampled for each support point from $\text{Exponential}(1/120)$, which gives an average storm lifetime of five days. Intensities, shapes, and velocities are sampled from the specified distributions with the hyperparameters given in Table 1. The values $m = 0.1, \phi = 1/2$ for the inverse Gaussian distribution on r gives an average speed of about 30 miles per hour. The parameter $q = 0.5$ places most of the mass on easterly storm tracks.

The value of the process $Y(x, t)$ is recorded at one million homogeneously spaced time points from $[0, T]$ at the five locations $\{x_1 = (5, 5), x_2 = (5, 5.5), x_3 = (1, 1), x_4 = (8, 8), x_5 = (3, 5)\}$, as well as twenty additional locations sampled uniformly on B . The five fixed points should result in the process at some pairs of locations being highly tail dependent, some pairs weakly dependent, and some nearly independent. After simulation, waiting times between exceedances of $y = \hat{F}_i^{-1}(0.99)$ and $y = \hat{F}_i^{-1}(0.999)$, where $\hat{F}_i^{-1}(\cdot)$ is the empirical distribution function of y_i , are calculated at the every unique pair of points. Mixture models of the form in (16) are then fit to the waiting times until first exceedance and the waiting times between exceedances at all pairs of locations.

Figure 2 shows results; some additional results are provided in Figure S2 in Supplementary Materials. The posterior concentrates around a single exponential component in the models for κ_i , which is consistent with the marginal distribution when $v = 0$ almost surely. Since most pairs of points are more distant than the product of storm velocity times lifetime, this near-independence result is sensible. Two components, and occasionally three, are required to model κ_Δ . At both thresholds, $\hat{\gamma}_d$ has a prominent mode near 0.05, and regardless of the choice of d , $\hat{\gamma}_d$ decreases with the distance between points. When $d = d_K$, for distances greater than about 2000 kilometers, $\hat{\gamma}_d$ is approximately 0.05. Notably, $\hat{\gamma}_d$ decays more slowly and exhibits substantially more variation when $d = \text{TV}$, suggesting possibly lower power for tests based on that metric.

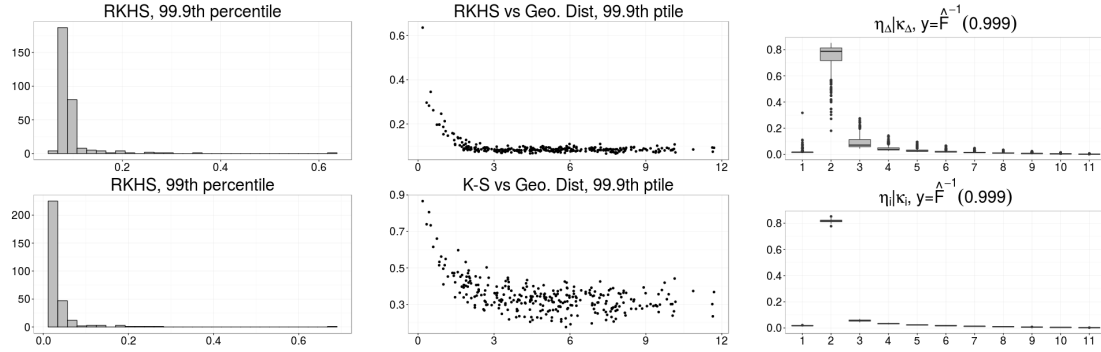


Figure 2: Left: histograms of $\hat{\gamma}_d$ for all pairs of locations with $d = d_K$ for thresholds $y_i = \hat{F}_i^{-1}(0.999)$ and $\hat{F}_i^{-1}(0.99)$. Center: plots of $\hat{\gamma}_d$ for $d = d_K$ and $d = \text{TV}$ for threshold $y_i = \hat{F}_i^{-1}(0.999)$ versus Euclidean distance between points. Right: Posterior estimates of $\eta_i | \kappa_i$ and $\eta_\Delta | \kappa_\Delta$ for $y = F^{-1}(0.999)$. Box plots are over all recorded points or all pairs of points.

5 Applications

The method is applied to four real data sets: (1) Daily precipitation data for 25 weather stations in the United States for the period 1940–2014; (2) Daily exchange rates for 12 currencies for the period

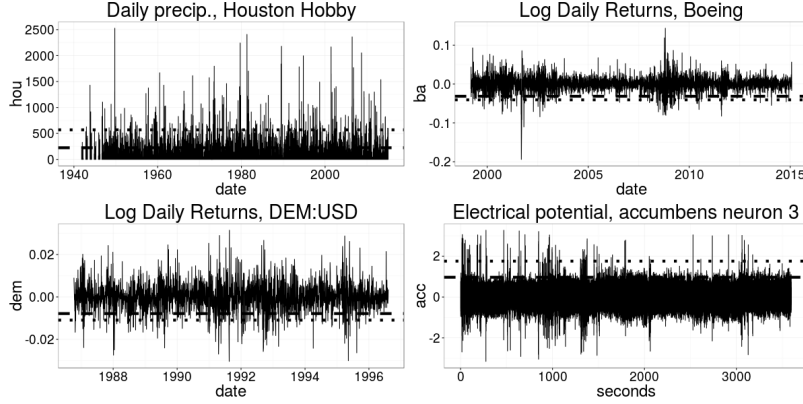


Figure 3: Examples of raw data $w(x, t)$. Dotted lines: more extreme threshold; dashed lines: less extreme threshold for computing γ_d .

1986–1996; (3) Daily prices for the period 2000–2014 of the 30 stocks that made up the Dow Jones Industrial Index as of January 2015; and (4) Electrical potential at 62 single neurons in the brain of a mouse exploring a maze, sampled at 500 Hz.

The first dataset is similar to the simulation study and the physical heuristic that we introduced in Section 2. The points in the max-stable velocity process can be thought of as storms or pressure systems in this context. The fourth—the mouse electrophysiology data—retains an explicit spatial component, as the physical distance between neurons is related to the speed at which signals can be propagated between them. The second and third applications are financial. One way to interpret the max stable velocity model in financial settings is to think of assets as embedded in latent space, with the distances between them reflecting similarity in the factors that determine their price. The support points of the process can be thought of as market sentiment, and their movement reflects the evolution of sentiment through the asset space. Larger values of u reflect panics—sentiments that affect many asset classes simultaneously—and large velocities reflects rapidly spreading sentiments. Finally, in financial settings it is usually extremes in the *left* tail that are of particular interest, and thus it is useful to model with max-stable velocity processes the negative of the observed data—so exceedances of the negative of a low threshold are the relevant events.

In choosing thresholds for analysis, the heuristic used is that at least 100 first exceedances of the highest threshold must be observed at all points. Thresholds correspond to empirical quantiles of the observed data, and at least two thresholds are analyzed for every dataset. A consequence of choosing thresholds in this way is that for some datasets, the empirical quantile of the chosen threshold may be much more extreme than for others. For example, the electrophysiology data has nearly two million observations, so we can choose thresholds of $y_i = \hat{F}_i^{-1}(0.998)$ or $y_i = \hat{F}_i^{-1}(0.99)$ for analysis; the exchange rate data has only about two thousand observations, so the thresholds chosen are $y_i = \hat{F}_i^{-1}(0.05)$ and $y_i = \hat{F}_i^{-1}(0.10)$. For the Dow Jones data, the thresholds are $y_i = \hat{F}_i^{-1}(0.025)$ and $\hat{F}_i^{-1}(0.05)$, and for the precipitation data, the thresholds are $y_i = \hat{F}_i^{-1}(0.99)$ and $y_i = \hat{F}_i^{-1}(0.95)$. Examples of single components of the four datasets are shown in Figure 3. In the case of the two financial datasets, the displayed series and data used for our analysis are the log daily returns $\log[w(x, t)/w(x, t - 1)]$, following standard practice in finance. The other two figures show the raw data plotted in the time domain.

For comparison, we use the method described in [14]. When W is in the max domain-of-attraction of a Brown-Resnick process, Engelke et al. [14] show that when the process is transformed to exponential margins, correlations in the increments of the process relative to its value any one location, conditional on threshold exceedance at the reference location, have approximately a Gaussian distribution. Practically, this approach proceeds by first transforming the data to have exponential margins. Label the transformed data $\tilde{w}(x, t)$, then choose a reference location and label it location 1. Compute the increments $\tilde{w}(\mathbf{x}_{[-1]}, t) - \tilde{w}(x_1, t)$ relative to location 1, where $\tilde{w}(\mathbf{x}_{[-1]}, t)$ is the vector of process realizations at time t at locations other than location 1. Retain only data points where $\tilde{w}(x_1, t)$ exceeds a high threshold. Now compute the correlations in $\tilde{w}(\mathbf{x}_{[-1]}, t) - \tilde{w}(x_1, t)$. The magnitude of the correlation provides inference on the strength of tail dependence; the closer the absolute correlation is to 1 or -1, the stronger the tail dependence. We refer to this as the conditional correlation method.

5.1 Precipitation

Results for analysis of the precipitation data are summarized in Figure 4. A map showing the location of each station can be found in Figure S1 in Supplementary Materials. Clear geographic structure is evident in the estimated values of γ_d . Similar geographic structure is seen in tail waiting times and conditional correlations. Overall, tail dependence is evident at nearby sites but decays with distance; for distances greater than about 500 km the estimated values of γ_d are all very similar. The number of exponential components in the models for κ_Δ and κ_i is almost always two, with κ_i having higher median weight on the second exponential component. This departs somewhat from the expected mixture of a single exponential component and an atom for a max-stable velocity process, but the discrete mixture model of (16) is still a good fit to the data.

5.2 Dow Jones components

Figure 5 shows results for analysis of negative log daily returns $-\log[w(x, t)/w(x, t-1)]$ for the DJIA data; the reference asset for the conditional correlations method is axp (American Express). Similar dependence structure is evident using the conditional correlation and tail waiting times methods. Most values of $\hat{\gamma}_d$ cluster around 0.2 at both thresholds, with a long right tail in the posterior point estimates. Here, unlike in the precipitation data, the posterior for the parameters of the mixture models for both κ_Δ and κ_i concentrated around three exponential components, albeit with most of the weight on the first two. This suggests that the data generating process is somewhat more complex than a simple max-stable velocity process. In particular, the max-stable velocity process is stationary in time, while financial returns often exhibit temporal nonstationarity. About half the assets pairs involving axp have values of $p_d > 0.95$. Notably, the largest values of $\hat{\gamma}_d$ for pairs involving axp are for jpm (JP Morgan Chase) and v (Visa), two other large credit card issuers. There is considerable dispersion in imputed waiting times, with a median of around eight days. A table showing the identity of the stock corresponding to each row/column in the colormaps in Figure 5 can be found in Table S2 in Supplementary Materials.

5.3 Exchange Rates

Exchange rate data for twelve currencies is described in [18] and [26]. Similar to the Dow Jones data, these series are transformed to negative log daily returns $(-\log[w(x, t)/w(x, t-1)])$ and analyzed

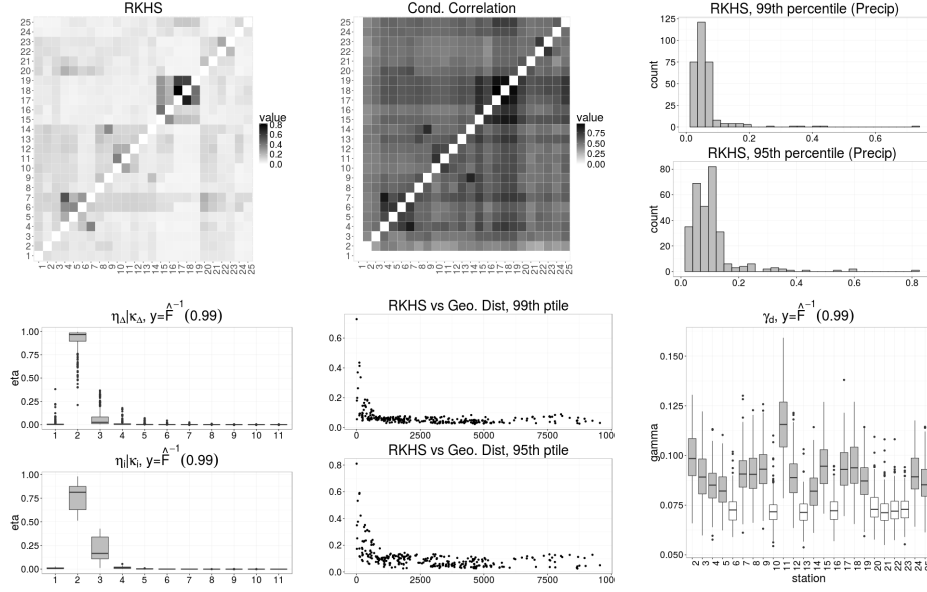


Figure 4: Results for daily precipitation data, $d = d_K$. Top Left: $\hat{\gamma}_d$ for thresholds $y_i = \hat{F}_i^{-1}(0.99)$ (below the main diagonal) and $y_i = \hat{F}_i^{-1}(0.95)$ (above the main diagonal). The sites are arranged by geographic distance. Top center: conditional correlations relative to site 1 $y_i = \hat{F}_i^{-1}(0.99)$ (below the main diagonal) and $y_i = \hat{F}_i^{-1}(0.95)$ (above the main diagonal). Top right: histograms of $\hat{\gamma}_d$ for both thresholds. Bottom left: box plots of posterior means of $\eta_d | \kappa_d$ (top) and $\eta_i | \kappa_i$ for $y_i = \hat{F}_i^{-1}(0.99)$. Bottom center: plots of $\hat{\gamma}_d$ versus geographic distance for both thresholds. Bottom right: box plot of posterior samples of γ_d for $y_i = -\hat{F}_i^{-1}(0.99)$ for pairs that include station 1, gray boxes indicate $p_d > 0.95$.

at two thresholds: $y_i = -\hat{F}_i^{-1}(0.05)$ and $y_i = -\hat{F}_i^{-1}(0.10)$. A table giving the full name of each currency and its corresponding row/column in the colormap is provided in Table S1 in Supplementary Materials. Figure 6 shows some results. Here, there is very clear structure in the pattern of pairwise dependence, with the European currencies (BEF, FRF, DEM, NLG, ESP, SEK, CHF, and GBP) showing strong evidence of dependence while the other four currencies (AUD, CAD, JPY, and NZD) show little evidence of tail dependence among themselves or with the European currencies. Results for the conditional correlation method were similar (not shown). The posterior intervals for γ_d —again, colored gray if $p_d > 0.95$ —show the same pattern, though notably all of the currencies have $p_d > 0.95$ for at least one pair. These results are broadly consistent with previous analysis of dependence at the mean in this dataset [see 26].

5.4 Electrophysiology

Potential data recorded at single neurons in the brain of a mouse interacting with a maze are described in [13] and analyzed here using two thresholds: $y_i = \hat{F}_i^{-1}(0.998)$ and $y_i = \hat{F}_i^{-1}(0.99)$. In electrophysiology, interest lies in modeling dependence between neuron “spikes” at different locations in the brain. Neuronal voltage spikes indicate transmission of signals along axonal pathways, and large potentials tend to cluster together in small time windows. These events are referred to as

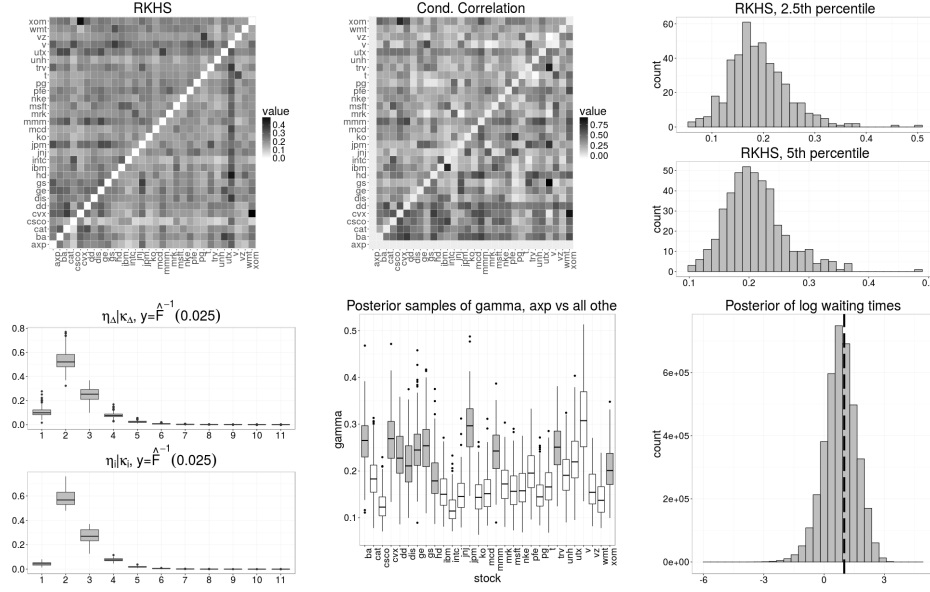


Figure 5: Results for DJIA components. Top Left: $\hat{\gamma}_d$ for thresholds $y_i = \hat{F}_i^{-1}(0.025)$ (below the main diagonal) and $y_i = \hat{F}_i^{-1}(0.05)$ (above the main diagonal). Top center: correlations conditional on exceedance of $y_i = \hat{F}_i^{-1}(0.025)$ (below the main diagonal) and $y_i = \hat{F}_i^{-1}(0.05)$ (above the main diagonal) by axp . Top right: histograms of $\hat{\gamma}_d$ for both thresholds. Bottom left: posterior means of $\eta_\Delta | \kappa_\Delta$ (top) and $\eta_i | \kappa_i$ for $y_i = \hat{F}_i^{-1}(0.99)$. Bottom center: posterior samples of γ_d for $y_i = -\hat{F}_i^{-1}(0.025)$ for pairs that include axp ; gray boxes indicate $p_d > 0.95$. Bottom right: samples of log imputed posterior waiting times (all pairs pooled) for exceedance of $y_i = -\hat{F}_i^{-1}(0.025)$; vertical line at ten days.

“spike trains.” Thus, in these data one expects to see extensive tail dependence, but the waiting times between spikes at different neurons are relevant, since they inform about the pathway that the signal takes through the brain.

The neurons are assigned to regions of the brain, which are shown in some of the subimages in Figure 7. There is ample evidence of strong tail dependence for most pairs of neurons. Four neurons show a markedly different pattern of dependence from the others: at times, electrodes are faulty, resulting in data quality problems, which is the most likely explanation. This anomaly aside, strong dependence is evident both from waiting times and conditional correlations approach. However, a pattern revealed by the waiting times method that is not as clear with conditional correlations is that γ_d increases markedly with y for almost every neuron pair. Moreover, clear differences in dependence between and within regions are evident using the waiting times approach, but less clear with the conditional correlation method. Mixture models for κ_i required three to four exponential components and those for κ_Δ between two and three, again suggesting that the data generating process may be nonstationary in time or otherwise more complex than a generic max-stable velocity process (for which two exponential components suffice). Posterior credible intervals for γ_d at $y = \hat{F}_i^{-1}(0.998)$ have $p_d > 0.95$ for all pairs involving the first Accumbens region neuron; this was largely the case for all 1891 pairs of neurons, indicating strong evidence of tail dependence across all brain regions.

The electrophysiology data are overall most similar to the Dow Jones data: values of γ_d are

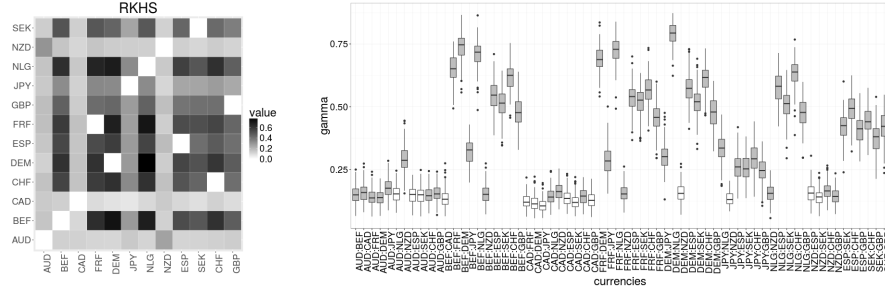


Figure 6: Results for exchange rate data. Left: $\hat{\gamma}_d$ for thresholds of (the negative of) $y_i = -\hat{F}_i^{-1}(0.05)$ (below the main diagonal) and $y_i = -\hat{F}_i^{-1}(0.10)$ (above the main diagonal). Right: box plot of posterior samples of γ_d for $y_i = -\hat{F}_i^{-1}(0.025)$ for all pairs of currencies. White boxes indicate $p_d > 0.95$

mostly large and increase as the threshold becomes more extreme. However, in these data the shift toward one in γ_d as y increases is much more prominent, with γ_d appearing almost uniformly distributed at $y_i = \hat{F}_i^{-1}(0.99)$ but massed near 1 at $y_i = \hat{F}_i^{-1}(0.999)$. Again, this shift is only evident using the waiting times method; it is not shown by conditional correlations.

6 Discussion

Characterizing tail dependence based on waiting times between peaks over thresholds has the advantage of greater flexibility and generality than existing alternatives in cases where temporal lags in extreme events are possible. The method relies strictly on the waiting times and inference on the parameter γ_d is relatively simple and computationally scalable, particularly when closed-form expressions are available for $d(\mu_\Delta, \mu_\Delta^\perp)$. The method has strong theoretical grounding in the class of max-stable velocity processes, which is sufficiently general to apply to distinct applications where extremal dependence is of interest. Broader classes of processes with non-trivial tail waiting times and classical tail dependence certainly exist. Modifying the max-stable velocity process to include time-varying magnitudes and velocities would create a much richer class of processes that retains the basic characteristics of the simpler process described here. Moreover, mixtures of the process could be devised to better model temporally nonstationary data that is common in financial and neuroscience applications.

The inferential method based on waiting times is robust to misspecification of the underlying process as long as the method selected for estimation of the waiting time distributions is sufficiently flexible. Here we have employed a Bayesian approach to estimating these densities based on discrete mixtures of exponentials and an atom at zero. This model appears to be sufficiently flexible in all of the applications considered here. It is not hard to conceive of fully nonparametric alternatives for situations in which the observed waiting time distributions are more complex, with the disadvantage of a possible loss of power.

Like other peaks-over-thresholds methods, our approach requires the choice of appropriate thresholds. Substantial work has been done on threshold choice for standard peaks-over-thresholds methods. It is unclear whether this will translate directly to threshold choice in this novel context. Here, we have taken the simpler approach of choosing multiple thresholds and attempting to infer a general pattern as the threshold changes. Further work on threshold choice is undoubtedly called for.

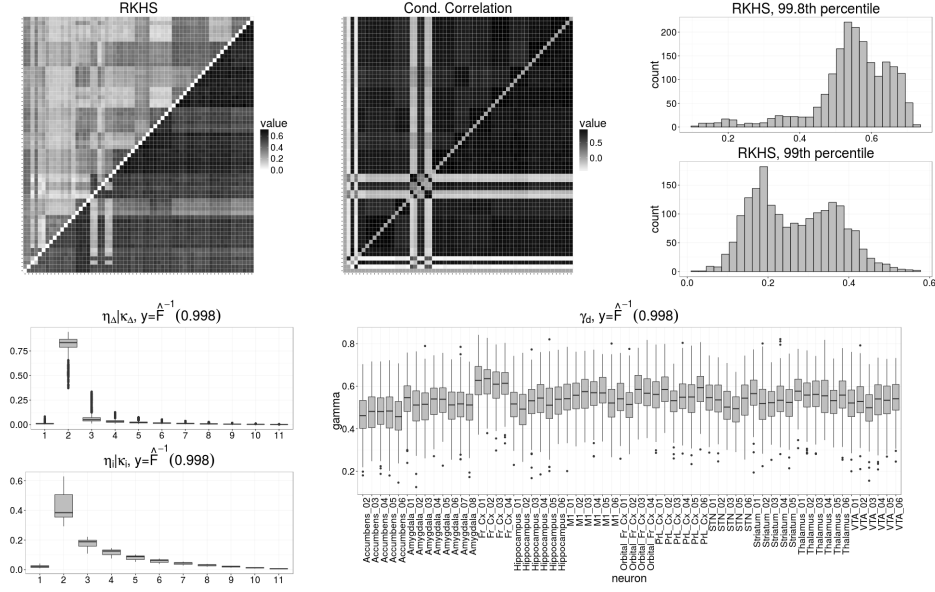


Figure 7: Results for electrophysiology data with $d = d_K$. Top left: $\hat{\gamma}_d$ for thresholds $y_i = \hat{F}_i^{-1}(0.998)$ (below the main diagonal) and $y_i = \hat{F}_i^{-1}(0.99)$ (above the main diagonal). Top center: correlations in increments relative to Accumbens 1, conditional on exceedance of $y_i = \hat{F}_i^{-1}(0.998)$ (below the main diagonal) and $y_i = \hat{F}_i^{-1}(0.99)$ (above the main diagonal) at Accumbens 1. Top right: histograms of γ_d for both thresholds across all pairs of neurons. Bottom left: $\eta_\Delta | \kappa_\Delta$ and $\eta_i | \kappa_i$ for $y = \hat{F}_i^{-1}(0.998)$. Bottom right: posterior samples of γ_d for $y_i = \hat{F}_i^{-1}(0.998)$ for all pairs that include Accumbens 1.

Additionally, we have thus far modeled the pairwise waiting times entirely independently; clear gains in estimation efficiency would result from sharing information across all pairs. These are promising areas for future work.

Acknowledgments

The authors thank Dan Cooley and David Dunson for helpful comments on drafts of this manuscript, and Kristian Lum for assistance in obtaining data for the climatological applications. James Johndrow acknowledges funding from the United States National Institute of Environmental Health Sciences, grant numbers ES017436, ES020619, and ES017240. Robert Wolpert acknowledges funding from United States National Science Foundation, grant numbers SES-1521855 and ACI-1550225.

Appendix

A Proof of Theorem 2.4 and Corollaries 2.6 and 2.5

A.1 Marginal Distribution of $Y(x, t)$

Fix $x \in \mathbb{R}^d$, $t \in \mathbb{R}$, and $y > 0$. Then the event

$$[Y(x, t) \leq y] = \{\mathcal{N}(A) = 0\}$$

that $Y(x, t)$ does not exceed y is identical to the event that the Poisson random measure $\mathcal{N}(d\omega)$ assigns zero points to the set

$$A = \{\omega : \sigma < t < \sigma + \tau, u\varphi_\Lambda(x - \xi - (t - \sigma)v) > y\}$$

of particles born before time t , surviving until time t , that move from their birth point ξ at velocity v to a location $\xi_t := \xi + (t - \sigma)v$ sufficiently close to x that their intensity u will lead to exceedance of level y . We will use $\nu(\cdot)$ to denote the measure of a set with respect to the intensity measure of \mathcal{N} . The probability of the event $\mathbb{P}(\mathcal{N}(A) = 0)$ for the Poisson measure $\mathcal{N} \sim \text{Po}(\nu(d\omega))$ is

$$\begin{aligned} \mathbb{P}[Y(x, t) \leq y] &= \exp(-\nu(A)) \\ &= \exp\left(-\int_{\mathbb{R}^d \times \mathcal{P}^d \times \mathbb{R}^d} \int_{\sigma < t < \sigma + \tau} \int_{u > y/\varphi_\Lambda(x - \xi_t)} u^{-2} du \beta \delta e^{-\delta \tau} d\tau d\sigma d\xi \pi(dv d\Lambda)\right) \\ &= \exp\left(-\int_{\mathbb{R}^d \times \mathcal{P}^d \times \mathbb{R}^d} \int_{\sigma < t < \sigma + \tau} \frac{1}{y} \varphi_\Lambda(x - \xi_t) \beta \delta e^{-\delta \tau} d\tau d\sigma d\xi \pi(dv d\Lambda)\right) \\ &= \exp\left(-\int_{\mathbb{R}^d \times \mathcal{P}^d \times \mathbb{R}^d} \frac{\beta}{\delta y} \varphi_\Lambda(x - \xi - (t - \sigma)v) d\xi \pi(dv d\Lambda)\right) \\ &= \exp\left(-\frac{\beta}{\delta y}\right), \end{aligned}$$

so $Y(x, t) \sim \text{Fr}(1, \beta/\delta)$ has the unit Fréchet distribution with scale β/δ for all locations $x \in \mathbb{R}^d$ and times $t > 0$, for any probability distribution $\pi(dv d\Lambda)$.

A.2 Marginal Distribution of κ and $Y^*(x, t)$

Now suppose that $\varphi(z)$ is a monotonically decreasing function of squared Euclidean length, and denote by $\xi_s := \xi + v(s - \sigma)$ the location at time $s \in \mathbb{R}$ of the particle $\omega = (u, \xi, \sigma, \tau, \Lambda, v)$, born at location ξ at time σ . The event that the first exceedance time $\kappa(y)$ of level $y > 0$ is later than any specified $t > 0$ is the event that the Poisson random measure $\mathcal{N}(d\omega)$ assigns zero points to the Borel set

$$A := \left\{ \omega : \sup_{s \in [0, t] \cap [\sigma, \sigma + \tau]} u\varphi_\Lambda(x - \xi_s) > y \right\}, \quad (18)$$

whose probability is $\mathbb{P}[\kappa(y) > t] = \exp(-\nu(A))$. It is convenient for us to write A as the disjoint union of several simpler pieces, and then sum their measures to find $\nu(A)$. For fixed $\Lambda \in \mathcal{P}^d$ and

$v \in \mathbb{R}^d$, denote by Δ the time interval (positive or negative) between birth and arrival at the closest point of approach to x (CPA), starting from ξ and traveling at velocity v , *i.e.*,

$$\begin{aligned}\Delta &:= \operatorname{argmax}_{s \in \mathbb{R}} \{\varphi_\Lambda(x - \xi - sv)\} \\ &= \operatorname{argmin}_{s \in \mathbb{R}} \{(x - \xi - sv)' \Lambda (x - \xi - sv)\} \\ &= v' \Lambda (x - \xi) / v' \Lambda v.\end{aligned}$$

Any vector $z \in \mathbb{R}^d$ can be written uniquely as the sum $z = (z^\parallel + z^\perp)$ of its projections onto the vector space spanned by the velocity vector v , and its orthogonal complement, in the inner product Λ , given by:

$$z^\parallel := (v' \Lambda z / v' \Lambda v) v \quad \quad \quad z^\perp := z - (v' \Lambda z / v' \Lambda v) v \quad (19)$$

The projection of $(x - \xi)$ onto the span of v is $(x - \xi)^\parallel = \Delta v$, and $\xi + \Delta v$ is the CPA to x .

The particle is initially *approaching* x if $v' \Lambda (x - \xi) > 0$, *i.e.*, $\Delta > 0$; otherwise it is initially *receding* from x . The supremum in (18) will be attained at time $s^* = \sigma + \Delta$, if that is in the interval $[0, t] \cap [\sigma, \sigma + \tau]$. If not, the supremum will be attained at one of the endpoints of that interval.

We write A as the disjoint union of five sets, one for each possible time

$$s^* = \operatorname{argmax} \{Y(x, s) : s \in [0, t] \cap [\sigma, \sigma + \tau]\}$$

at which $Y(x, s)$ attains its maximum in $[0, t]$: the beginning $s = 0$ or end $s = t$ of the interval, the time of the particle's birth $s = \sigma$ or death $s = \sigma + \tau$, or some intermediate point.

A_1 : $s^* \in (0, t) \cap (\sigma, \sigma + \tau)$. The particle initially approaches x (*i.e.*, $\Delta > 0$) and reaches CPA before its death or time t , whichever occurs first. The supremum $\sup_s [\varphi_\Lambda(x - \xi_s)]$ occurs at CPA time $s^* = \sigma + \Delta$, at which time $\xi_{s^*} = \xi + \Delta v$ so

$$(x - \xi_{s^*}) = x - \xi - \Delta v = (x - \xi)^\perp,$$

the projection of $(x - \xi)$ onto the orthogonal complement of v . It follows that

$$A_1 = \{\omega : u \varphi_\Lambda(x - \xi_{s^*}) > y, \quad (0 \vee \sigma) \leq (\sigma + \Delta) \leq (t \wedge (\sigma + \tau))\} \quad (20)$$

After integrating wrt $u^{-2} du$,

$$\nu(A_1) = \frac{1}{y} \int_{\mathbb{R}^d \times \mathcal{P}^d \times \mathbb{R}^d \times (-\Delta \leq \sigma \leq t - \Delta) \times (\Delta \leq \tau < \infty)} \mathbf{1}_{\{\Delta > 0\}} \beta \delta e^{-\delta \tau} \varphi_\Lambda(x - \xi_{s^*}) \, d\tau d\sigma d\xi \pi(dv \, d\Lambda)$$

Integrating wrt τ , then σ ,

$$= \frac{\beta}{y} t \int_{\mathbb{R}^d \times \mathcal{P}^d \times \mathbb{R}^d} \mathbf{1}_{\{\Delta > 0\}} e^{-\delta \Delta} \varphi_\Lambda((x - \xi)^\perp) \, d\xi \pi(dv \, d\Lambda)$$

Changing variables from ξ to (Δ, ζ) with $\Delta = v' \Lambda (x - \xi) / v' \Lambda v$ (so $\Delta v = (x - \xi)^\parallel$) and $\zeta = (x - \xi)^\perp \in v^\perp \equiv \mathbb{R}^{d-1}$, with Jacobian $|v| = \sqrt{v' \Lambda v}$, and integrating wrt Δ ,

$$= \frac{\beta}{\delta y} t \int_{\mathbb{R}^d \times \mathcal{P}^d \times \{\zeta \in v^\perp\}} \varphi_\Lambda(\zeta) \, d\zeta |v| \pi(dv \, d\Lambda). \quad (21)$$

A_2 : $s^* = t$. The particle approaches x and survives until time t but fails to reach CPA by t . The supremum $\sup_s [\varphi_\Lambda(x - \xi_s)]$ occurs at time $s^* = t$, at which time $\xi_{s^*} = \xi + (t - \sigma)v$:

$$A_2 = \{\omega : u\varphi_\Lambda(x - \xi - (t - \sigma)v) > y, \quad (0 \vee \sigma) \leq t < \sigma + (\tau \wedge \Delta)\} \quad (22)$$

After integrating wrt $u^{-2}du$, and noting that $(x - \xi_{s^*}) = (x - \xi)^\perp + (\Delta - (t - \sigma))v$ so the $d\xi$ integral extends over the half-space on which $v'\Lambda(x - \xi_{s^*}) > 0$,

$$\begin{aligned} \nu(A_2) &= \frac{1}{y} \int_{\mathbb{R}^d \times \mathcal{P}^d \times (-\infty, t] \times (t - \sigma, \infty) \times \mathbb{R}^d} \mathbf{1}_{\{\Delta > t - \sigma\}} \beta \delta e^{-\delta \tau} \varphi_\Lambda(x - \xi_{s^*}) \, d\xi \, d\tau \, d\sigma \, \pi(dv \, d\Lambda) \\ &= \frac{1}{2y} \int_{\mathbb{R}^d \times \mathcal{P}^d \times (-\infty, t] \times (t - \sigma, \infty)} \beta \delta e^{-\delta \tau} \, d\tau \, d\sigma \, \pi(dv \, d\Lambda) \\ &= \frac{1}{2y} \int_{(-\infty, t] \times (t - \sigma, \infty)} \beta \delta e^{-\delta \tau} \, d\tau \, d\sigma \\ &= \frac{\beta}{2\delta y}. \end{aligned} \quad (23)$$

A_3 : $s^* = \sigma + \tau$. The particle lives to time 0 and approaches x but dies before time t without reaching the CPA. The supremum $\sup_s [\varphi_\Lambda(x - \xi_s)]$ occurs at death time $s^* = \sigma + \tau$, at which time $\xi_{s^*} = \xi + \tau v$, so

$$A_3 = \{\omega : u\varphi_\Lambda(x - \xi - \tau v) > y, \quad (0 \vee \sigma) \leq \sigma + \tau \leq t \wedge (\sigma + \Delta)\} \quad (24)$$

After integrating wrt $u^{-2}du$, and noting that $(x - \xi_{s^*}) = (x - \xi)^\perp + (\Delta - \tau)v$ so the $d\xi$ integral extends over the half-space on which $v'\Lambda(x - \xi_{s^*}) > 0$,

$$\begin{aligned} \nu(A_3) &= \frac{1}{y} \int_{\mathbb{R}^d \times \mathcal{P}^d \times (0, \infty) \times (-\tau, t - \tau) \times \mathbb{R}^d} \mathbf{1}_{\{\Delta > \tau\}} \beta \delta e^{-\delta \tau} \varphi_\Lambda(x - \xi - \tau v) \, d\xi \, d\sigma \, d\tau \, \pi(dv \, d\Lambda) \\ &= \frac{1}{2y} \int_{\mathbb{R}^d \times \mathcal{P}^d \times (0, \infty) \times (-\tau, t - \tau)} \beta \delta e^{-\delta \tau} \, d\sigma \, d\tau \, \pi(dv \, d\Lambda) \\ &= \frac{1}{2y} \int_{(0, \infty) \times (-\tau, t - \tau)} \beta \delta e^{-\delta \tau} \, d\sigma \, d\tau \\ &= \frac{\beta}{2\delta y} \, \delta t. \end{aligned} \quad (25)$$

A_4 : $s^* = 0$. The particle is born before time zero, and by time zero is still alive and is receding from x (either because it receded initially, or because it passed the CPA before time zero). Because this system is invariant under time-reversal, this set has the same ν measure as the set A_2 , giving $\nu(A_4) = \beta(2\delta y)^{-1}$.

A_5 : $s^* = \sigma$. The particle was born during the interval $[0, t]$ and recedes from x . Again appealing to time-reversibility, $\nu(A_5) = \nu(A_3) = \beta(2\delta y)^{-1}$.

A.3 Summary

The ν measures of the five pieces are:

$$\begin{aligned}\nu(A_1) &= \frac{\beta}{\delta y} t \int_{\mathbb{R}^d \times \mathcal{P}^d \times \{\zeta \in v^\perp\}} \varphi_\Lambda(\zeta) d\zeta |v| \pi(dv d\Lambda) \\ \nu(A_2) &= \frac{\beta}{2\delta y} \quad \nu(A_3) = \frac{\beta}{2\delta y} \delta t \quad \nu(A_4) = \frac{\beta}{2\delta y} \quad \nu(A_5) = \frac{\beta}{2\delta y} \delta t\end{aligned}$$

whose sum is

$$\nu(A) = \frac{\beta}{\delta y} \left\{ 1 + \delta t + t \int_{\mathbb{R}^d \times \mathcal{P}^d \times \{\zeta \in v^\perp\}} \varphi_\Lambda(\zeta) d\zeta |v| \pi(dv d\Lambda) \right\}. \quad (26)$$

Thus, the probability distribution of the first time $\kappa(y)$ that $Y(x, t)$ exceeds any level y is of the form

$$\mathbb{P}[\kappa(y) > t] = \exp(-\nu(A)) = \exp\left(-\frac{\beta}{\delta y} - t \cdot \text{const}\right), \quad (27)$$

a mixture of a point-mass at zero of magnitude $1 - \exp(\beta/\delta y)$ and an exponentially-distributed random variable whose rate constant

$$\frac{\beta}{\delta y} \left\{ \delta + \int_{\mathbb{R}^d \times \mathcal{P}^d \times v^\perp} \varphi_\Lambda(\zeta) d\zeta |v| \pi(dv d\Lambda) \right\}$$

depends on the mean particle speed and kernel shape. Corollary 2.5 follows immediately since $[Y^*(x, t) < y]$ and $[\kappa(y) > t]$ are identical events.

A.4 Special Case: Gaussian Kernel

Consider the Gaussian case of $\varphi(z) = (2\pi)^{-d/2} \exp(-z'z/2)$, and fix any $\Lambda \in \mathcal{P}^d$ and $v \in \mathbb{R}^d$. The projection of $\xi \in \mathbb{R}^d$ onto the span of v (see (19)) is $\xi^\parallel = (v'\Lambda\xi/v'\Lambda v)v = \Delta v$, where $\Delta = (v'\Lambda\xi/v'\Lambda v)$, with squared Λ -length $(\xi^\parallel)'\Lambda(\xi^\parallel) = \Delta^2 v'\Lambda v$. Using (38)

$$\int_{v^\perp} \varphi_\Lambda(\zeta) d\zeta |v| = (v'\Lambda v/2\pi)^{\frac{1}{2}},$$

and $\nu(A)$ from (26) is

$$\nu(A) = \frac{\beta}{\delta y} \left\{ 1 + \delta t + t \int_{\mathbb{R}^d \times \mathcal{P}^d} (v'\Lambda v/2\pi)^{\frac{1}{2}} \pi(dv d\Lambda) \right\}. \quad (28)$$

B Proof of Theorem 2.7

Applying the inclusion-exclusion principle and change-of-variables from ξ to $z := (\xi - v\sigma)$ to (8a) gives the result.

C Proof of Theorem 2.11

In this section we compute a lower bound for the probability of two exceedances $Y(x_j, s_j) > y_j$, $j = 1, 2$ of levels $\{y_j\} \subset \mathbb{R}_+$ at locations $\{x_j\} \subset \mathbb{R}^d$ within the interval $\{s_j\} \subset [0, t]$ for $t > 0$. Some calculations used in the sequel are found in Section D.

C.1 General case

We consider the case in which CPA is attained at both points during the interval $[0, t]$ for the general max-stable velocity process. For $j = 1, 2$ set:

$$\begin{aligned}\Delta_j &:= \operatorname{argmax}_{s \in \mathbb{R}} \{ \varphi_\Lambda(x_j - \xi - sv) \} = v' \Lambda(x_j - \xi) / v' \Lambda v \\ s_j^* &:= \operatorname{argmax}_{s \in [0, t] \cap [\sigma, \sigma + \tau]} \{ \varphi_\Lambda(x_j - \xi - (s - \sigma)v) \} \\ u_j^* &:= \frac{y_j}{\varphi_\Lambda(x_j - \xi_{s_j^*})}.\end{aligned}$$

To achieve exceedance and CPA at both locations a particle must satisfy

$$u > u_1^* \vee u_2^* \quad s_j^* = \sigma + \Delta_j \in [0, t] \cap [\sigma, \sigma + \tau], \quad j = 1, 2. \quad (29)$$

Write the set $A \subset \Omega$ of particles that satisfy these conditions as the union of four sets

$$A_{ij} := \{ \omega \in \Omega : \Delta_i = (\Delta_1 \wedge \Delta_2), \quad u_j^* = (u_1^* \vee u_2^*) \} \quad i, j = 1, 2 \quad (30)$$

characterized by which CPA occurs first and which exceedance requires the larger mass u . For example,

$$A_{11} = \{ \omega \in \Omega : u > u_1^* > u_2^*, (0 \vee \sigma) < \sigma + \Delta_1 < \sigma + \Delta_2 < t \wedge (\sigma + \tau) \}$$

consists of the particles that initially approach both x_1 and x_2 and reach CPA for both before their death. Both suprema $\sup_s [\varphi_\Lambda(x - \xi_s)]$ occur at the CPA times $s_j^* = \sigma + \Delta_j$, at CPA locations $\xi_{s_j^*} = \xi + \Delta_j v$, so

$$(x_j - \xi_{s_j^*}) = (x_j - \xi - \Delta_j v) = (x_j - \xi)^\perp$$

is the projection of $(x_j - \xi)$ onto the orthogonal complement of v for $j = 1, 2$. After integrating wrt $u^{-2} du$, we have

$$\nu(A_{11}) = \frac{1}{y_1} \int_{\substack{\mathbb{R}^d \times \mathcal{P}^d \times \mathbb{R}^d \\ \times (-\Delta_1 < \sigma < t - \Delta_2) \\ \times (\Delta_2 < \tau < \infty)}} \mathbf{1}_{\{0 < \Delta_1 < \Delta_2\}} \mathbf{1}_{\{u_1^* > u_2^*\}} \beta \delta e^{-\delta \tau} \varphi_\Lambda((x_1 - \xi)^\perp) d\tau d\sigma d\xi \pi(dv d\Lambda)$$

Integrating with respect to τ then σ ,

$$\begin{aligned}&= \frac{\beta}{y_1} \int_{\mathbb{R}^d \times \mathcal{P}^d \times \mathbb{R}^d} (t - (\Delta_2 - \Delta_1)) e^{-\delta \Delta_2} \varphi_\Lambda((x_1 - \xi)^\perp) \times \\ &\quad \mathbf{1}_{\{0 < \Delta_1 < \Delta_2\}} \mathbf{1}_{\{\Delta_2 - \Delta_1 \leq t\}} \mathbf{1}_{\{u_1^* > u_2^*\}} d\xi \pi(dv d\Lambda).\end{aligned} \quad (31)$$

Change variables from $\xi \in \mathbb{R}^d$ to $(\zeta, \gamma) \in v^\perp \times v^\parallel$ with

$$\zeta := \left(\frac{x_1 + x_2}{2} - \xi \right)^\perp, \quad \gamma := \left(\frac{x_1 + x_2}{2} - \xi \right)^\parallel$$

and introduce the quantity

$$\Delta_{12} := (\Delta_2 - \Delta_1) = v' \Lambda (x_2 - x_1) / v' \Lambda v,$$

noting that it doesn't depend on ξ . With this we can write

$$\Delta_1 = -\frac{1}{2}\Delta_{12} + v' \Lambda \gamma / v' \Lambda v \quad \Delta_2 = +\frac{1}{2}\Delta_{12} + v' \Lambda \gamma / v' \Lambda v.$$

Introduce $\mu := \frac{1}{2}(x_2 - x_1)^\perp$ and note that

$$\varphi_\Lambda(x_1 - \xi_{s_j}^*) = \varphi_\Lambda((x_1 - \xi)^\perp) = \varphi_\Lambda(\zeta - \mu) \quad (32a)$$

$$\varphi_\Lambda(x_2 - \xi_{s_j}^*) = \varphi_\Lambda((x_2 - \xi)^\perp) = \varphi_\Lambda(\zeta + \mu) \quad (32b)$$

The limits imposed by the indicator functions in (31) are:

$$\begin{aligned} 0 \leq \Delta_2 - \Delta_1 \leq t &\Leftrightarrow 0 \leq v' \Lambda (x_2 - x_1) \leq t v' \Lambda v \\ 0 \leq \Delta_1 &\Leftrightarrow \Delta_{12} v' \Lambda v \leq 2 v' \Lambda \gamma \\ u_2^* \leq u_1^* &\Leftrightarrow \varphi_\Lambda(\zeta - \mu) / \varphi_\Lambda(\zeta + \mu) \leq y_1 / y_2 \end{aligned}$$

Rewriting (31) with this variable change, then integrating wrt γ , gives

$$\begin{aligned} \nu(A_{11}) &= \frac{\beta}{y_1} \int_{\mathbb{R}^d \times \mathcal{P}^d \times v^\perp \times v^\parallel} (t - \Delta_{12}) e^{-\delta \Delta_{12} / 2 - \delta v' \Lambda \gamma / v' \Lambda v} \varphi_\Lambda(\zeta - \mu) \times \\ &\quad \mathbf{1}_{\{0 \leq v' \Lambda (x_2 - x_1) \leq t v' \Lambda v\}} \mathbf{1}_{\{\Delta_{12} v' \Lambda v \leq 2 v' \Lambda \gamma\}} \mathbf{1}_{\{\varphi_\Lambda(\zeta - \mu) / \varphi_\Lambda(\zeta + \mu) \leq y_1 / y_2\}} d\gamma d\zeta \pi(dv d\Lambda) \\ &= \frac{\beta}{\delta y_1} \int_{\mathbb{R}^d \times \mathcal{P}^d} (t - \Delta_{12}) e^{-\delta \Delta_{12}} \mathbf{1}_{\{0 \leq v' \Lambda (x_2 - x_1) \leq t v' \Lambda v\}} \times \\ &\quad \left\{ \int_{\zeta \in v^\perp: \frac{\varphi_\Lambda(\zeta - \mu)}{\varphi_\Lambda(\zeta + \mu)} \leq \frac{y_1}{y_2}} \varphi_\Lambda(\zeta - \mu) d\zeta \right\} |v| \pi(dv d\Lambda). \end{aligned} \quad (33)$$

Now, we find the measure of the other three sets. First

$$A_{21} = \{\omega \in \Omega : u > u_2^* > u_1^*, (0 \vee \sigma) < \sigma + \Delta_1 < \sigma + \Delta_2 < t \wedge (\sigma + \tau)\},$$

giving

$$\begin{aligned} \nu(A_{21}) &= \frac{\beta}{\delta y_2} \int_{\mathbb{R}^d \times \mathcal{P}^d} (t - \Delta_{12}) e^{-\delta \Delta_{12}} \mathbf{1}_{\{0 \leq v' \Lambda (x_2 - x_1) \leq t v' \Lambda v\}} \times \\ &\quad \left\{ \int_{\zeta \in v^\perp: \frac{\varphi_\Lambda(\zeta - \mu)}{\varphi_\Lambda(\zeta + \mu)} \geq \frac{y_1}{y_2}} \varphi_\Lambda(\zeta + \mu) d\zeta \right\} |v| \pi(dv d\Lambda). \end{aligned} \quad (34)$$

Finally, it is clear that with

$$A_{12} = \{\omega \in \Omega : u > u_1^* > u_2^*, (0 \vee \sigma) < \sigma + \Delta_2 < \sigma + \Delta_1 < t \wedge (\sigma + \tau)\}$$

$$A_{22} = \{\omega \in \Omega : u > u_2^* > u_1^*, (0 \vee \sigma) < \sigma + \Delta_2 < \sigma + \Delta_1 < t \wedge (\sigma + \tau)\}$$

we have

$$\begin{aligned} \nu(A_{12}) &= \frac{\beta}{\delta y_1} \int_{\mathbb{R}^d \times \mathcal{P}^d} (t + \Delta_{12}) e^{\delta \Delta_{12}} \mathbf{1}_{\{0 \leq -v' \Lambda(x_2 - x_1) \leq t v' \Lambda v\}} \times \\ &\quad \left\{ \int_{\zeta \in v^\perp : \frac{\varphi_\Lambda(\zeta - \mu)}{\varphi_\Lambda(\zeta + \mu)} \leq \frac{y_1}{y_2}} \varphi_\Lambda(\zeta - \mu) d\zeta \right\} |v| \pi(dv d\Lambda). \\ \nu(A_{22}) &= \frac{\beta}{\delta y_2} \int_{\mathbb{R}^d \times \mathcal{P}^d} (t + \Delta_{12}) e^{\delta \Delta_{12}} \mathbf{1}_{\{0 \leq -v' \Lambda(x_2 - x_1) \leq t v' \Lambda v\}} \times \\ &\quad \left\{ \int_{\zeta \in v^\perp : \frac{\varphi_\Lambda(\zeta - \mu)}{\varphi_\Lambda(\zeta + \mu)} \geq \frac{y_1}{y_2}} \varphi_\Lambda(\zeta + \mu) d\zeta \right\} |v| \pi(dv d\Lambda). \end{aligned}$$

C.2 Gaussian case

Now take $\varphi(z) = (2\pi)^{-d/2} \exp(-z'z/2)$ and fix $v, \Lambda \in \mathbb{R}^d \times \mathcal{P}^d$. The set of $\zeta \in v^\perp$ over which the bracketed integral in (33) is taken can be written as:

$$\begin{aligned} \varphi_\Lambda(\zeta - \mu) &\leq \frac{y_1}{y_2} \varphi_\Lambda(\zeta + \mu) \\ -\frac{1}{2}(\zeta - \mu)' \Lambda (\zeta - \mu) &\leq \log \frac{y_1}{y_2} - \frac{1}{2}(\zeta + \mu)' \Lambda (\zeta + \mu) \\ \mu' \Lambda \zeta &\leq \frac{1}{2} \log \frac{y_1}{y_2} \end{aligned}$$

Writing $\zeta \in v^\perp$ as the sum $\zeta = \zeta_\perp + \zeta_\parallel$ of components orthogonal and parallel to $(x_2 - x_1)^\perp$ (in the Λ metric), by (41),

$$\nu(A_{11}) = \frac{\beta}{y_1} \int_{\substack{\mathbb{R}^d \times \mathcal{P}^d \\ 0 \leq \Delta_{12} \leq t}} (t - \Delta_{12}) e^{-\delta \Delta_{12}} \sqrt{v' \Lambda v / 2\pi} \Phi\left(-\frac{S_\Lambda^\perp(v)}{2} + \frac{\log(y_1/y_2)}{S_\Lambda^\perp(v)}\right) \pi(dv d\Lambda).$$

with $S_\Lambda^\perp(v) := \{(x_2 - x_1)' \Lambda (x_2 - x_1)^\perp\}^{1/2}$. The other three sets have measure

$$\begin{aligned} \nu(A_{21}) &= \frac{\beta}{y_2} \int_{\substack{\mathbb{R}^d \times \mathcal{P}^d \\ 0 \leq \Delta_{12} \leq t}} (t - \Delta_{12}) e^{-\delta \Delta_{12}} \sqrt{v' \Lambda v / 2\pi} \Phi\left(-\frac{S_\Lambda^\perp(v)}{2} - \frac{\log(y_1/y_2)}{S_\Lambda^\perp(v)}\right) \pi(dv d\Lambda). \\ \nu(A_{12}) &= \frac{\beta}{y_1} \int_{\substack{\mathbb{R}^d \times \mathcal{P}^d \\ 0 \leq -\Delta_{12} \leq t}} (t + \Delta_{12}) e^{\delta \Delta_{12}} \sqrt{v' \Lambda v / 2\pi} \Phi\left(-\frac{S_\Lambda^\perp(v)}{2} + \frac{\log(y_1/y_2)}{S_\Lambda^\perp(v)}\right) \pi(dv d\Lambda). \\ \nu(A_{22}) &= \frac{\beta}{y_2} \int_{\substack{\mathbb{R}^d \times \mathcal{P}^d \\ 0 \leq -\Delta_{12} \leq t}} (t + \Delta_{12}) e^{\delta \Delta_{12}} \sqrt{v' \Lambda v / 2\pi} \Phi\left(-\frac{S_\Lambda^\perp(v)}{2} - \frac{\log(y_1/y_2)}{S_\Lambda^\perp(v)}\right) \pi(dv d\Lambda). \end{aligned}$$

Recognizing a simple change of variables, we have

$$\nu(A) = \frac{\beta}{\sqrt{2\pi}} \int_{\substack{\mathbb{R}^d \times \mathcal{P}^d \\ \cap \{-t \leq \Delta_{12} \leq t\}}} (t - \Delta_{12}) e^{-\delta \Delta_{12}} \left\{ \frac{1}{y_1} \Phi\left(-\frac{S_\Lambda^\perp(v)}{2} + \frac{\log(y_1/y_2)}{S_\Lambda^\perp(v)}\right) \right.$$

$$+ \frac{1}{y_2} \Phi \left(-\frac{S_{\Lambda}^{\perp}(v)}{2} - \frac{\log(y_1/y_2)}{S_{\Lambda}^{\perp}(v)} \right) \Big\} \sqrt{v' \Lambda v} \pi(dv d\Lambda)$$

where $A = A_{11} \cup A_{12} \cup A_{21} \cup A_{22}$. So

$$\begin{aligned} \mathbb{P}[|\kappa_2 - \kappa_1| > t] &\leq 1 - \mathbb{P}[\kappa_1 \vee \kappa_2 \leq t] \\ &\leq 1 - \mathbb{P}[\text{CPA Exceedances at } x_1, x_2 \text{ in } [0, t]] \\ &\leq \exp\{-\nu(A)\}, \end{aligned}$$

so the probability $\mathbb{P}[|\kappa_2 - \kappa_1| > t] \rightarrow 0$ as $\mathbb{E}_{\pi} \left[\sqrt{v' \Lambda v} \Phi \left(-\sqrt{(x_2 - x_1)' \Lambda (x_2 - x_1)^{\perp}} \right) \right] \rightarrow \infty$.

D Some Important Integrals

As before, fix $v, x_1, x_2, \xi \in \mathbb{R}^d$ and $\Lambda \in \mathcal{P}^d$, and set

$$\Delta_j := v' \Lambda (x_i - \xi) \quad \Delta_{12} := (\Delta_2 - \Delta_1) = v' \Lambda (x_2 - x_1) \quad \mu := \frac{1}{2}(x_2 - x_1)^{\perp}$$

where, as before, for any $z \in \mathbb{R}^d$ we denote the projections of z parallel and orthogonal to v in the Λ metric by

$$z^{\parallel} := (v' \Lambda z / v' \Lambda v) v \quad z^{\perp} = z - z^{\parallel}$$

and the value of the kernel function at z by

$$\varphi_{\Lambda}(z) := |\Lambda/2\pi|^{\frac{1}{2}} \exp(-z' \Lambda z/2)$$

Then

$$\begin{aligned} \int_{\mathbb{R}^d} \exp(-\tfrac{1}{2} \xi' \Lambda \xi) d\xi &= |\Lambda/2\pi|^{\frac{1}{2}} \\ \int_{v^{\parallel}} \exp(-\tfrac{1}{2} \gamma' \Lambda \gamma) d\gamma &= \int_{\mathbb{R}} \exp(-s^2 v' \Lambda v/2) |v| ds \end{aligned} \tag{35}$$

with the CoV $\gamma = sv$ with Jacobian $d\gamma = \sqrt{v' v} ds$

$$= (v' \Lambda v/2\pi)^{-\frac{1}{2}} |v| \tag{36}$$

$$\begin{aligned} \int_{v^{\perp}} \exp(-\tfrac{1}{2} \zeta' \Lambda \zeta) d\zeta &= \text{the ratio of (35)/(36)} \\ &= |\Lambda/2\pi|^{\frac{1}{2}} (v' \Lambda v/2\pi)^{\frac{1}{2}} / |v|, \text{ so} \end{aligned} \tag{37}$$

$$\int_{v^{\perp}} \varphi_{\Lambda}(\zeta) d\zeta = (v' \Lambda v/2\pi)^{\frac{1}{2}} / |v|. \tag{38}$$

$$\begin{aligned} \int_{\mu^{\parallel}} \exp(-\tfrac{1}{2} w' \Lambda w) dw &= \int_{\mathbb{R}} \exp(-s^2 \mu' \Lambda \mu/2) |\mu| ds \\ &= (\mu' \Lambda \mu/2\pi)^{-\frac{1}{2}} |\mu| \end{aligned} \tag{39}$$

$$\begin{aligned}
\int_{\{v,\mu\}^\perp} \exp\left(-\frac{1}{2}q'\Lambda q\right) dq &= \text{the ratio of (37)/(39)} \\
&= |\Lambda/2\pi|^{\frac{1}{2}} (v'\Lambda v \mu'\Lambda\mu)^{\frac{1}{2}} / 2\pi |v| |\mu|, \text{ so} \\
\int_{\{v,\mu\}^\perp} \varphi_\Lambda(\zeta) d\zeta &= (v'\Lambda v \mu'\Lambda\mu)^{\frac{1}{2}} / 2\pi |v| |\mu|. \tag{40}
\end{aligned}$$

If the integral in (39) extends only over those $\zeta \in \mu^\parallel$ with $\mu'\Lambda\zeta \leq \frac{1}{2} \log(y_1/y_2)$, its value is reduced by a factor of $\Phi\left(\frac{\log(y_1/y_2) - 2\mu'\Lambda\mu}{2\sqrt{\mu'\Lambda\mu}}\right)$, leading to

$$\int_{v^\perp} \varphi_\Lambda(\zeta - \mu) \mathbf{1}_{\{\mu'\Lambda\zeta \geq \frac{1}{2} \log(y_1/y_2)\}} d\zeta = \Phi\left(\frac{\frac{1}{2} \log \frac{y_1}{y_2} - \mu'\Lambda\mu}{\sqrt{\mu'\Lambda\mu}}\right) \left(\frac{v'\Lambda v}{2\pi v'v}\right)^{\frac{1}{2}}. \tag{41}$$

References

- [1] Balkema, G. and Embrechts, P. (2007). *High risk scenarios and extremes: a geometric approach*. European Mathematical Society.
- [2] Ballani, F. and Schlather, M. (2011). A construction principle for multivariate extreme value distributions. *Biometrika*, 98(3):633–645.
- [3] Beguería, S., Angulo-Martínez, M., Vicente-Serrano, S. M., López-Moreno, J. I., and El-Kenawy, A. (2011). Assessing trends in extreme precipitation events intensity and magnitude using non-stationary peaks-over-threshold analysis: a case study in northeast Spain from 1930 to 2006. *International Journal of Climatology*, 31(14):2102–2114.
- [4] Beguería, S. and Vicente-Serrano, S. M. (2006). Mapping the hazard of extreme rainfall by peaks over threshold extreme value analysis and spatial regression techniques. *Journal of applied meteorology and climatology*, 45(1):108–124.
- [5] Beirlant, J., Goegebeur, Y., Segers, J., and Teugels, J. (2006). *Statistics of extremes: theory and applications*. John Wiley & Sons.
- [6] Buishand, T. A., de Haan, L., and Zhou, C. (2008). On spatial extremes: with application to a rainfall problem. *The Annals of Applied Statistics*, pages 624–642.
- [7] Coles, S., Bawa, J., Trenner, L., and Dorazio, P. (2001). *An introduction to statistical modeling of extreme values*, volume 208. Springer.
- [8] Coles, S. G. and Tawn, J. A. (1991). Modelling extreme multivariate events. *Journal of the Royal Statistical Society. Series B (Methodological)*, 53(2):377–392.
- [9] Das, B. and Resnick, S. I. (2011). Conditioning on an extreme component: Model consistency with regular variation on cones. *Bernoulli*, 17(1):226–252.
- [10] Davison, A. C. and Smith, R. L. (1990). Models for exceedances over high thresholds. *Journal of the Royal Statistical Society. Series B (Methodological)*, 52(3):393–442.
- [11] de Haan, L. (1984). A spectral representation for max-stable processes. *The Annals of Probability*, 12(4):1194–1204.

- [12] de Haan, L. and Ferreira, A. (2006). *Extreme value theory: an introduction*. Springer Science & Business Media.
- [13] Dzirasa, K., Phillips, H. W., Sotnikova, T. D., Salahpour, A., Kumar, S., Gainetdinov, R. R., Caron, M. G., and Nicolelis, M. A. L. (2010). Noradrenergic control of cortico-striato-thalamic and mesolimbic cross-structural synchrony. *The Journal of Neuroscience*, 30(18):6387–6397.
- [14] Engelke, S., Malinowski, A., Kabluchko, Z., and Schlather, M. (2014). Estimation of Hüsler–Reiss distributions and Brown–Resnick processes. *Journal of the Royal Statistical Society: Series B (Statistical Methodology)*, 77(1):239–265.
- [15] Ghosal, S., Ghosh, J. K., and Van Der Vaart, A. W. (2000). Convergence rates of posterior distributions. *Annals of Statistics*, 28(2):500–531.
- [16] Gretton, A., Borgwardt, K. M., Rasch, M., Schölkopf, B., and Smola, A. J. (2006). A kernel method for the two-sample-problem. In *Advances in neural information processing systems*, pages 513–520.
- [17] Gretton, A., Borgwardt, K. M., Rasch, M. J., Schölkopf, B., and Smola, A. (2012). A kernel two-sample test. *The Journal of Machine Learning Research*, 13(1):723–773.
- [18] Harrison, J. and West, M. (1999). *Bayesian Forecasting & Dynamic Models*. Springer.
- [19] Heffernan, J. E. and Resnick, S. I. (2007). Limit laws for random vectors with an extreme component. *The Annals of Applied Probability*, 17(2):537–571.
- [20] Heffernan, J. E. and Tawn, J. A. (2004). A conditional approach for multivariate extreme values (with discussion). *Journal of the Royal Statistical Society: Series B (Statistical Methodology)*, 66(3):497–546.
- [21] Heffernan, J. E., Tawn, J. A., and Zhang, Z. (2007). Asymptotically (in) dependent multivariate maxima of moving maxima processes. *Extremes*, 10(1-2):57–82.
- [22] Katz, R. W., Parlange, M. B., and Naveau, P. (2002). Statistics of extremes in hydrology. *Advances in water resources*, 25(8):1287–1304.
- [23] Meinguet, T. (2012). Maxima of moving maxima of continuous functions. *Extremes*, 15(3):267–297.
- [24] Méndez, F. J., Menéndez, M., Luceño, A., and Losada, I. J. (2006). Estimation of the long-term variability of extreme significant wave height using a time-dependent peak over threshold (POT) model. *Journal of Geophysical Research: Oceans*, 111(C7).
- [25] Minsker, S., Srivastava, S., Lin, L., and Dunson, D. B. (2014). Robust and scalable Bayes via a median of subset posterior measures. *arXiv preprint arXiv:1403.2660*.
- [26] Prado, R. and West, M. (2010). *Time series: modeling, computation, and inference*. CRC Press.
- [27] Resnick, S. I. and Roy, R. (1991). Random usc functions, max-stable processes and continuous choice. *The Annals of Applied Probability*, pages 267–292.

- [28] Rootzén, H. and Tajvidi, N. (2006). Multivariate generalized Pareto distributions. *Bernoulli*, 12(5):917–930.
- [29] Rousseau, J. and Mengersen, K. (2011). Asymptotic behaviour of the posterior distribution in overfitted mixture models. *Journal of the Royal Statistical Society: Series B (Statistical Methodology)*, 73(5):689–710.
- [30] Schlather, M. (2002). Models for stationary max-stable random fields. *Extremes*, 5(1):33–44.
- [31] Smith, R. L. (1984). Threshold methods for sample extremes. In *Statistical extremes and applications*, pages 621–638. Springer.
- [32] Smith, R. L. (1989). Extreme value analysis of environmental time series: an application to trend detection in ground-level ozone. *Statistical Science*, 4(4):367–377.
- [33] Smith, R. L. (1990). Max-stable processes and spatial extremes. *Unpublished manuscript, University of Surrey*.
- [34] Smith, R. L. and Weissman, I. (1996). Characterization and estimation of the multivariate extremal index. *UNC working papers*.
- [35] Smola, A., Gretton, A., Song, L., and Schölkopf (2007). Hilbert space embeddings for distributions. In *Proceedings of the 18th International Conference on Algorithmic Learning*, pages 18–31. Springer.
- [36] Song, L., Huang, J., Smola, A., and Fukumizu, K. (2009). Hilbert space embeddings of conditional distributions with applications to dynamical systems. In *Proceedings of the 26th Annual International Conference on Machine Learning*, pages 961–968. ACM.
- [37] Sriperumbudur, B. K., Gretton, A., Fukumizu, K., Schölkopf, B., and Lanckriet, G. R. G. (2010). Hilbert space embeddings and metrics on probability measures. *The Journal of Machine Learning Research*, 11:1517–1561.
- [38] Tawn, J. A. (1988). Bivariate extreme value theory: models and estimation. *Biometrika*, 75(3):397–415.
- [39] Tawn, J. A. (1990). Modelling multivariate extreme value distributions. *Biometrika*, 77(2):245–253.
- [40] Zhang, Z. and Smith, R. L. (2010). On the estimation and application of max-stable processes. *Journal of Statistical Planning and Inference*, 140(5):1135–1153.

Supplementary Materials

S1 Proof of Theorems 2.2 and 2.3

S1.1 Proof of Theorem 2.2

Theorem 2.2 is a corollary of the following result.

Theorem S1.1 (Maxima of MSV Processes). *If $Y_i \stackrel{\text{iid}}{\sim} \text{MSV}(\beta, \delta, \pi, \varphi)$ are independent MSV processes for $1 \leq i \leq n$ then their maximum $\vee_{1 \leq i \leq n} Y_i(x, t) := \max_{1 \leq i \leq n} Y_i(x, t)$ is a max-stable velocity process with the $\text{MSV}(n\beta, \delta, \pi, \varphi)$ distribution.*

Proof. Each of $\{Y_i\}$ has a representation (4a) for the support points $\{\omega_j^{(i)}\}_{j \in \mathbb{N}}$ of the i th of n independent Poisson random measures $\mathcal{N}^{(i)}(d\omega) \stackrel{\text{iid}}{\sim} \text{Po}(\nu(du))$ for the intensity measure $\nu(d\omega)$ of (3). Then their sum $\mathcal{N}^+(d\omega) := \sum_{1 \leq i \leq n} \mathcal{N}^{(i)}(d\omega) \sim \text{Po}(n\nu(du))$ is also a Poisson random measure, with intensity measure n times $\nu(d\omega)$ and with support equal to the union of the supports of $\{\mathcal{N}^{(i)}\}$. The MSV processes associated with \mathcal{N}^+ is precisely $\vee_{1 \leq i \leq n} Y_i(x, t)$, since

$$\begin{aligned} \mathbb{P}[\vee_{1 \leq i \leq n} Y_i(x, t) < y] &= \mathbb{P}[\cap_{i=1}^n \{Y_i < y\}] \\ &= \prod_{i=1}^n e^{-\nu(B)} = e^{-n\nu(B)}, \end{aligned}$$

for $B = \{Y_i < y\}$. But the measure $n \cdot \nu$ of (3) is exactly that of the $\text{MSV}(n\beta, \delta, \pi, \varphi)$ process. \square

We now prove Theorem 2.2.

Proof. Fix $Y \sim \text{MSV}(\beta, \delta, \pi, \varphi)$ and n iid max-stable copies $\{Y_i\}_{1 \leq i \leq n} \stackrel{\text{iid}}{\sim} \text{MSV}(\beta, \delta, \pi, \varphi)$. By Theorem S1.1 the maximum $\vee_{1 \leq i \leq n} Y_i(x, t)$ has the $\text{MSV}(n\beta, \delta, \pi, \varphi)$ distribution. By (8) in Theorem 2.7, multiply β and each y_j by n to see that all finite-dimensional marginal joint distributions of $\{\vee_{1 \leq i \leq n} Y_i(x, t)\}$ are identical to those of $\{nY(x, t)\}$, so $Y(x, t) \stackrel{\mathcal{D}}{=} \frac{1}{n} \vee_{1 \leq i \leq n} Y_i(x, t)$ satisfies (1) of Theorem 2.1 and Y is max-stable. \square

S1.2 Proof of Theorem 2.3

We first prove two lemmas used in obtaining the main result.

Lemma S1.1. *If $Y_1 \sim \text{MSV}(\beta, \delta, \pi, \varphi)$ and $Y_c \sim \text{MSV}(c\beta, \delta, \pi, \varphi)$ for some $c > 0$, then $cY_1^* \stackrel{\mathcal{D}}{=} Y_c^*$.*

Proof.

Fix $\{x_i\}_{1 \leq i \leq n} \subset \mathbb{R}^d$ and $\{t_i\}_{1 \leq i \leq n} \subset \mathbb{R}$. The joint CDF for $\{Y_1^*(x_i, t_i)\}$ at $\{y_i\} \subset \mathbb{R}_+$ is

$$\mathbb{P}[\cap_{1 \leq i \leq n} [Y_1^*(x_i, t_i) \leq y_i]] = \exp(-\nu(\cup_{1 \leq i \leq n} A_i)) \quad (\text{S.1})$$

for the exceedance events $A_i := [Y_1^*(x_i, t_i) > y_i]$, which may be written

$$A_i = \left\{ \omega : u > \frac{y_i}{\sup_{(0 \vee \sigma) \leq s \leq (t_i \wedge \sigma + \tau)} \{\varphi_\Lambda(x_i - \xi - v(s - \sigma))\}} \right\}.$$

By the inclusion-exclusion principle, $\nu(\cup A_i)$ can be evaluated as

$$\nu(\cup_{1 \leq i \leq n} A_i) = \sum_{\emptyset \neq J \subset \{1, \dots, n\}} (-1)^{1+|J|} \nu(\cap_{j \in J} A_j), \quad (\text{S.2})$$

where $|J|$ denotes the cardinality of J . For a finite set $J \subset \{1, \dots, n\}$ of indices, the intersection

$$\bigcap_{j \in J} A_j = \left\{ \omega : u > \max_{j \in J} \left[\frac{y_j}{\sup_{(0 \vee \sigma) \leq s \leq (t_j \wedge \sigma + \tau)} \{\varphi_\Lambda(x_j - \xi - v(s - \sigma))\}} \right] \right\}$$

has ν -measure (after changing variables from ξ to $z := \xi + v\sigma$)

$$\nu\left(\bigcap_{j \in J} A_j\right) = \int \min_{j \in J} \left[\frac{\sup_{(0 \vee \sigma) \leq s \leq (t_j \wedge \sigma + \tau)} \{\varphi_\Lambda(x_j - vs - z)\}}{y_j} \right] dz \beta d\sigma \delta e^{-\delta\tau} d\tau \pi(dv d\Lambda) \quad (\text{S.3})$$

The measure $\nu(\cap_{j \in J} A_j)$ in (S.3) is unchanged if both β and each y_j are multiplied by the same constant $c > 0$. By (S.2), the $\nu(\cup_{1 \leq i \leq n} A_i)$ is also unchanged.

Finally, by (S.1) and (S.3),

$$\begin{aligned} \mathbb{P}[\cap_{1 \leq i \leq n} [c Y_1^*(x_i, t_i) \leq y_i]] &= \mathbb{P}\left[\bigcap_{1 \leq i \leq n} [Y_1^*(x_i, t_i) \leq y_i/c]\right] \\ &= \mathbb{P}\left[\bigcap_{1 \leq i \leq n} [Y_c^*(x_i, t_i) \leq y_i]\right], \end{aligned}$$

proving the lemma. \square

Lemma S1.2. *If $\{Y_i\}_{1 \leq i \leq n} \stackrel{\text{iid}}{\sim} \text{MSV}(\beta, \delta, \pi, \varphi)$ are independent MSV processes with maximal processes*

$$Y_i^*(x, t) := \sup_{0 \leq s \leq t} Y_i(x, s), \quad t > 0$$

then the maximum $\vee_{1 \leq i \leq n} Y_i^(x, t)$ is the maximal process $Y^*(x, t)$ for a max-stable velocity process $Y \sim \text{MSV}(n\beta, \delta, \pi, \varphi)$.*

Proof.

Each of $\{Y_i\}$ has a representation (4a) for the support points $\{\omega_j^{(i)}\}_{j \in \mathbb{N}}$ of the i th of n independent Poisson random measures $\mathcal{N}^{(i)}(d\omega) \stackrel{\text{iid}}{\sim} \text{Po}(\nu(du))$ for the intensity measure $\nu(d\omega)$ of (3). The sum $\mathcal{N}^+(d\omega) := \sum_{1 \leq i \leq n} \mathcal{N}^{(i)}(d\omega) \sim \text{Po}(n\nu(du))$ is also a Poisson random measure, with intensity

measure $n\nu(d\omega)$ and with support equal to the union $\{\omega_j^{(i)}\}$ of the supports of $\{\mathcal{N}^{(i)}\}$, and the max-stable velocity process $Y(x, t)$ associated with $\mathcal{N}^+(d\omega)$ by (4a) is $\vee_{1 \leq i \leq n} Y_i(x, t)$. By Theorem S1.1, $Y \sim \text{MSV}(n\beta, \delta, \pi, \varphi)$. But $\vee_{1 \leq i \leq n} Y_i^*(x, t) = Y^*(x, t)$ and the Lemma follows. \square

We now prove Theorem 2.3.

Proof.

Let $\{Y_i\}_{1 \leq i \leq n} \stackrel{\text{iid}}{\sim} \text{MSV}(\beta, \delta, \pi, \varphi)$ and $Y \sim \text{MSV}(\beta, \delta, \pi, \varphi)$ be independent MSV processes with maximal processes

$$Y_i^*(x, t) := \sup_{0 \leq s \leq t} Y_i(x, s) \quad Y^*(x, t) := \sup_{0 \leq s \leq t} Y(x, s), \quad t > 0$$

By Lemma S1.2, there exists a process $Y_0 \sim \text{MSV}(n\beta, \delta, \pi, \varphi)$ whose maximal process Y_0^* is the maximum $\vee_{1 \leq i \leq n} Y_i^*(x, t)$. By Lemma S1.1 with $c = n$, $Y_0^* \stackrel{\mathcal{D}}{=} n Y^*$, i.e., $Y^*(x, t) \stackrel{\mathcal{D}}{=} \frac{1}{n} \vee_{1 \leq i \leq n} Y_i^*(x, t)$. By (1) in Theorem 2.1, $Y^*(x, t)$ is max-stable. \square

S2 Proof of Corollary 2.8

By Theorem 2.7, the joint CDF of $Y_{t_1}(x_1)$ and $Y_{t_2}(x_2)$ can be found as

$$\mathbb{P}[Y_{t_1}(x_1) \leq y_1, Y_{t_2}(x_2) \leq y_2] = \exp(-\nu(A_1 \cup A_2))$$

for the sets

$$A_i := \{\omega : \sigma < t_i < \sigma + \tau, u\varphi_\Lambda(x_i - \xi - (t_i - \sigma)v) > y_i\}$$

of particles leading to an exceedance of y_i at (x_i, t_i) for $i = 1, 2$. In Theorem 2.4, we found $\nu(A_i) = \beta/\delta y_i$. To find the required $\nu(A_1 \cup A_2) = \nu(A_1) + \nu(A_2) - \nu(A_1 \cap A_2)$ we need the measure of the intersection. Putting $\xi_{t_i} = \xi + (t_i - \sigma)v$,

$$\begin{aligned} \nu(A_1 \cap A_2) &= \int_{\mathcal{P}^d \times \mathbb{R}^d \times \mathbb{R}^d} \int_{\sigma \leq (t_1 \wedge t_2)} \int_{\tau \geq (t_1 \vee t_2) - \sigma} \int_{u \geq \left(\frac{y_1}{\varphi_\Lambda(x_1 - \xi_{t_1})} \vee \frac{y_2}{\varphi_\Lambda(x_2 - \xi_{t_2})} \right)} u^{-2} du \delta e^{-\delta\tau} d\tau \beta d\sigma d\xi \pi(dv d\Lambda) \\ &= \int_{\mathcal{P}^d \times \mathbb{R}^d \times \mathbb{R}^d} \int_{\sigma \leq (t_1 \wedge t_2)} \int_{\tau \geq (t_1 \vee t_2) - \sigma} \left(\frac{\varphi_\Lambda(x_1 - \xi_{t_1})}{y_1} \wedge \frac{\varphi_\Lambda(x_2 - \xi_{t_2})}{y_2} \right) \delta e^{-\delta\tau} d\tau \beta d\sigma d\xi \pi(dv d\Lambda) \\ &= \int_{\mathcal{P}^d \times \mathbb{R}^d \times \mathbb{R}^d} \int_{\sigma \leq (t_1 \wedge t_2)} \left(\frac{\varphi_\Lambda(x_1 - \xi_{t_1})}{y_1} \wedge \frac{\varphi_\Lambda(x_2 - \xi_{t_2})}{y_2} \right) e^{-\delta((t_1 \vee t_2) - \sigma)} \beta d\sigma d\xi \pi(dv d\Lambda) \end{aligned}$$

Set

$$\Delta_v := (x_2 - x_1) - (t_2 - t_1)v \tag{S.4}$$

(which doesn't depend on σ) and change variables from ξ to $z := \xi - \frac{x_1+x_2}{2} + v[\frac{t_1+t_2}{2} - \sigma]$:

$$\begin{aligned} &= \int_{\mathcal{P}^d \times \mathbb{R}^d \times \mathbb{R}^d} \int_{\sigma \leq (t_1 \wedge t_2)} \left(\frac{\varphi_\Lambda(z - \Delta_v/2)}{y_1} \wedge \frac{\varphi_\Lambda(z + \Delta_v/2)}{y_2} \right) \\ &\quad e^{-\delta((t_1 \vee t_2) - \sigma)} \beta d\sigma dz \pi(dv d\Lambda) \\ &= \frac{\beta}{\delta} e^{-\delta|t_2-t_1|} \int_{\mathcal{P}^d \times \mathbb{R}^d \times \mathbb{R}^d} \left(\frac{\varphi_\Lambda(z - \Delta_v/2)}{y_1} \wedge \frac{\varphi_\Lambda(z + \Delta_v/2)}{y_2} \right) dz \pi(dv d\Lambda), \end{aligned} \quad (\text{S.5})$$

so then

$$\begin{aligned} \nu(A_1 \cup A_2) &= \frac{\beta}{\delta} \left[\frac{1}{y_1} + \frac{1}{y_2} \right] \\ &\quad - \frac{\beta}{\delta} e^{-\delta|t_2-t_1|} \int_{\mathcal{P}^d \times \mathbb{R}^d \times \mathbb{R}^d} \left(\frac{\varphi_\Lambda(z - \Delta_v/2)}{y_1} \wedge \frac{\varphi_\Lambda(z + \Delta_v/2)}{y_2} \right) dz \pi(dv d\Lambda) \end{aligned}$$

In the Gaussian case with $\varphi(z) = (2\pi)^{-d/2} \exp(-z'z/2)$ this simplifies. Set $B_1 := A_1 \cap A_2 \cap \{\omega : \Delta' \Lambda z < \log \frac{y_1}{y_2}\}$, the set of $\omega \in A_1 \cap A_2$ where the minimum in (S.5) is attained at (x_1, t_1) , and set $B_2 = (A_1 \cap A_2) \setminus B_1$, the set on which it is attained at (x_2, t_2) . Then

$$\nu(B_1) = \frac{\beta}{\delta y_1} e^{-\delta|t_2-t_1|} \int_{\mathcal{P}^d \times \mathbb{R}^d \times \mathbb{R}^d} \varphi_\Lambda(z - \Delta_v/2) \mathbf{1}_{\{\Delta' \Lambda z < \log \frac{y_1}{y_2}\}} dz \pi(dv d\Lambda)$$

For fixed v let $\zeta := z - (\Delta'_v \Lambda z / \Delta'_v \Lambda \Delta_v) \Delta_v$ be the orthogonal projection onto the space Δ_v^\perp perpendicular to Δ_v in the Λ norm, and change variables from z to (ζ, s) with $z = \zeta + s \Delta_v$ and Jacobian $dz = (\Delta'_v \Delta_v)^{\frac{1}{2}} d\zeta ds$, to find

$$\begin{aligned} \nu(B_1) &= \frac{\beta}{\delta y_1} e^{-\delta|t_2-t_1|} \int_{\mathcal{P}^d \times \mathbb{R}^d \times \Delta_v^\perp \times \mathbb{R}} |\Lambda/2\pi|^{\frac{1}{2}} \exp(-\zeta' \Lambda \zeta/2) e^{-s^2 \Delta'_v \Lambda \Delta_v/2} \\ &\quad \mathbf{1}_{\{s < \log \frac{y_1}{y_2} / \Delta'_v \Lambda \Delta_v\}} \sqrt{\Delta'_v \Delta_v} ds d\zeta \pi(dv d\Lambda) \\ &= \frac{\beta}{\delta y_1} e^{-\delta|t_2-t_1|} \int_{\mathcal{P}^d \times \mathbb{R}^d} \Phi\left(\frac{\log \frac{y_1}{y_2}}{S_\Lambda(v)} - \frac{1}{2} S_\Lambda(v)\right) \pi(dv d\Lambda) \end{aligned}$$

where $S_\Lambda(v) := \sqrt{\Delta'_v \Lambda \Delta_v}$. Similarly,

$$\begin{aligned} \nu(B_2) &= \frac{\beta}{\delta y_2} e^{-\delta|t_2-t_1|} \int_{\mathcal{P}^d \times \mathbb{R}^d} \Phi\left(\frac{\log \frac{y_2}{y_1}}{S_\Lambda(v)} - \frac{1}{2} S_\Lambda(v)\right) \pi(dv d\Lambda), \quad \text{so} \\ \nu(A_1 \cap A_2) &= \nu(B_1) + \nu(B_2) = \frac{\beta}{\delta} e^{-\delta|t_2-t_1|} \int_{\mathcal{P}^d \times \mathbb{R}^d} \left\{ \frac{1}{y_1} \Phi\left(\frac{\log \frac{y_1}{y_2}}{S_\Lambda(v)} - \frac{1}{2} S_\Lambda(v)\right) + \right. \\ &\quad \left. + \frac{1}{y_2} \Phi\left(\frac{\log \frac{y_2}{y_1}}{S_\Lambda(v)} - \frac{1}{2} S_\Lambda(v)\right) \right\} \pi(dv d\Lambda) \end{aligned}$$

and

$$\nu(A_1 \cup A_2) = \frac{\beta}{\delta} \left(\frac{1}{y_1} + \frac{1}{y_2} \right) - \nu(A_1 \cap A_2)$$

$$\begin{aligned}
&= \frac{\beta}{\delta} \left(1 - e^{-\delta|t_2-t_1|}\right) \left(\frac{1}{y_1} + \frac{1}{y_2}\right) \\
&+ \frac{\beta}{\delta} e^{-\delta|t_2-t_1|} \int_{\mathcal{P}^d \times \mathbb{R}^d} \left\{ \frac{1}{y_1} \Phi\left(\frac{1}{2}S_\Lambda(v) - \frac{\log \frac{y_1}{y_2}}{S_\Lambda(v)}\right) + \right. \\
&\quad \left. + \frac{1}{y_2} \Phi\left(\frac{1}{2}S_\Lambda(v) - \frac{\log \frac{y_2}{y_1}}{S_\Lambda(v)}\right) \right\} \pi(dv d\Lambda). \tag{S.6}
\end{aligned}$$

S3 Proof of Theorem 2.9

For $a_i, b_i \geq 0$ let κ_1, κ_2 be independent nonnegative random variables satisfying

$$\mathbb{P}[\kappa_i > t] = \exp(-a_i - b_i t), \quad t > 0$$

and set $\kappa_\Delta := |\kappa_1 - \kappa_2|$. Then for $t > 0$,

$$\begin{aligned}
\mathbb{P}[\kappa_\Delta > t] &= (1 - e^{-a_1})e^{-a_2-b_2t} && \kappa_1 = 0 < t < \kappa_2 \\
&+ (1 - e^{-a_2})e^{-a_1-b_1t} && \kappa_2 = 0 < t < \kappa_1 \\
&+ \int_{\mathbb{R}_+} b_1 \exp(-a_1 - b_1x_1 - a_2 - b_2(x_1+t)) dx_1 && 0 < \kappa_1 < \kappa_1+t < \kappa_2 \\
&+ \int_{\mathbb{R}_+} b_2 \exp(-a_2 - b_2x_2 - a_1 - b_1(x_2+t)) dx_2 && 0 < \kappa_2 < \kappa_2+t < \kappa_1
\end{aligned}$$

or, combining terms,

$$\begin{aligned}
\mathbb{P}[\kappa_\Delta > t] &= (1 - e^{-a_2})e^{-a_1-b_1t} + (1 - e^{-a_1})e^{-a_2-b_2t} \\
&+ \frac{b_2e^{-a_1-a_2}}{b_1+b_2}e^{-b_1t} + \frac{b_1e^{-a_1-a_2}}{b_1+b_2}e^{-b_2t} \\
&= \left\{ \frac{b_1e^{-a_1-a_2}}{b_1+b_2} + e^{-a_1}(1 - e^{-a_2}) \right\} e^{-b_1t} + \left\{ \frac{b_2e^{-a_1-a_2}}{b_1+b_2} + e^{-a_2}(1 - e^{-a_1}) \right\} e^{-b_2t}.
\end{aligned}$$

Thus κ_Δ is distributed as a mixture with three components: a point mass at zero and two exponential distributions with rates b_1 and b_2 . From (6) we have

$$a_i = \frac{\beta}{\delta y_i} \quad b_i = \frac{\beta}{\delta y_i} \left\{ \delta + \int_{\mathbb{R}^d \times \mathcal{P}^d \times v^\perp} \varphi_\Lambda(\zeta) d\zeta |v| \Pi(d\Lambda dv) \right\}$$

S4 Proof of Theorem 2.10

We first calculate the measures of three sets:

B_0 : the set where one or more support points is alive between time 0 and time t that causes an exceedance of y_1 at x_1 and y_2 at x_2 .

B_1 : the set where one or more support points is alive between time 0 and time t that causes an exceedance of y_1 at x_1 but no support points are alive during this time that cause an exceedance of y_2 at x_2 .

B_2 : the set where one or more support points is alive between time 0 and time t that causes an exceedance of y_2 at x_2 but no support points are alive during this time that cause an exceedance of y_1 at x_1 .

These measures will then be used to derive the waiting time distribution with zero velocity. As usual $\omega = (u, \xi, \sigma, \tau, a) \in \Omega$ will be used to denote a generic support point, with attribute $a = (v, \Lambda)$. Recall that, since $v \equiv 0$ and $\pi(\{0\} \times \mathcal{P}^d) = 1$, we are abusing notation and writing the marginal distribution of Λ as “ $\pi(d\Lambda)$ ”.

S4.1 Evaluating $\nu(B_0)$

The set B_0 consists of those $\omega \in \Omega$ for which $Y(x_1, s) > y_1$ and $Y(x_2, s) > y_2$ for some $0 \leq s \leq t$, leading to a simultaneous exceedance and $\kappa_\Delta = 0$. The time of the simultaneous occurrence will necessarily be $s = 0$, if $Y(x_1, 0) > y_1$ and $Y(x_2, 0) > y_2$, and otherwise $s = \sigma \in (0, t]$. The probability of a contemporaneous exceedance in the interval $[0, t]$ is $\exp(-\nu(B_0))$, with

$$\begin{aligned} \nu(B_0) &= \nu \left\{ \omega : u > \frac{y_1}{\varphi_\Lambda(x_1 - \xi)} \vee \frac{y_2}{\varphi_\Lambda(x_2 - \xi)}, \quad -\tau < \sigma \leq t \right\} \\ &= \int_\Omega \mathbf{1}_{\{u > [\frac{y_1}{\varphi_\Lambda(x_1 - \xi)} \vee \frac{y_2}{\varphi_\Lambda(x_2 - \xi)}]\}} \mathbf{1}_{\{-\tau < \sigma \leq t\}} u^{-2} du d\xi \beta d\sigma \delta e^{-\delta\tau} d\tau \pi(d\Lambda) \\ &= \int_{\mathbb{R} \times \mathbb{R}_+} \mathbf{1}_{\{-\tau < \sigma \leq t\}} \beta d\sigma \delta e^{-\delta\tau} d\tau \times \\ &\quad \times \int_{\mathbb{R}^d \times \mathcal{P}^d} \left[\frac{\varphi_\Lambda(x_1 - \xi)}{y_1} \wedge \frac{\varphi_\Lambda(x_2 - \xi)}{y_2} \right] d\xi \pi(d\Lambda) \\ &= \frac{\beta}{\delta} (1 + \delta t) \int_{\mathbb{R}^d \times \mathcal{P}^d} \left[\frac{\varphi_\Lambda(x_1 - \xi)}{y_1} \wedge \frac{\varphi_\Lambda(x_2 - \xi)}{y_2} \right] d\xi \pi(d\Lambda) \\ &= \frac{\beta}{\delta} (1 + \delta t) \int_{\mathbb{R}^d \times \mathcal{P}^d} \left[\frac{1}{y_1} \mathbf{1}_{\{\frac{\varphi_\Lambda(z)}{\varphi_\Lambda(z + \Delta_0)} < \frac{y_1}{y_2}\}} + \frac{1}{y_2} \mathbf{1}_{\{\frac{\varphi_\Lambda(z)}{\varphi_\Lambda(z - \Delta_0)} < \frac{y_2}{y_1}\}} \right] \varphi_\Lambda(z) dz \pi(d\Lambda) \end{aligned}$$

for $\Delta_0 = (x_2 - x_1)$ as in (S.4), with $v = 0$.

S4.2 Evaluating $\nu(B_1)$ and $\nu(B_2)$

The set B_1 consists of those $\omega \in \Omega$ for which $Y(x_1, s) > y_1$ for some $0 \leq s \leq t$ but $Y(x_2, s) \leq y_2$ for all $0 \leq s \leq t$. The probability that this exceedance pattern does not occur is $\exp(-\nu(B_1))$, with

$$\begin{aligned} \nu(B_1) &= \nu \left\{ \omega : \frac{y_1}{\varphi_\Lambda(x_1 - \xi)} < u \leq \frac{y_2}{\varphi_\Lambda(x_2 - \xi)}, \quad -\tau < \sigma \leq t \right\} \\ &= \int_\Omega \mathbf{1}_{\{\frac{y_1}{\varphi_\Lambda(x_1 - \xi)} < u \leq \frac{y_2}{\varphi_\Lambda(x_2 - \xi)}\}} \mathbf{1}_{\{-\tau < \sigma \leq t\}} u^{-2} du d\xi \beta d\sigma \delta e^{-\delta\tau} d\tau \pi(d\Lambda) \\ &= \int_{\mathbb{R} \times \mathbb{R}_+} \mathbf{1}_{\{-\tau < \sigma \leq t\}} \beta d\sigma \delta e^{-\delta\tau} d\tau \times \end{aligned}$$

$$\begin{aligned}
& \times \int_{\mathbb{R}^d \times \mathcal{P}^d} \left[\frac{\varphi_\Lambda(x_1 - \xi)}{y_1} - \frac{\varphi_\Lambda(x_2 - \xi)}{y_2} \right] \mathbf{1}_{\left\{ \frac{\varphi_\Lambda(x_2 - \xi)}{\varphi_\Lambda(x_1 - \xi)} < \frac{y_2}{y_1} \right\}} d\xi \pi(d\Lambda) \\
&= \frac{\beta}{\delta} (1 + \delta t) \int_{\mathbb{R}^d \times \mathcal{P}^d} \left[\frac{\varphi_\Lambda(x_1 - \xi)}{y_1} - \frac{\varphi_\Lambda(x_2 - \xi)}{y_2} \right] \mathbf{1}_{\left\{ \frac{\varphi_\Lambda(x_2 - \xi)}{\varphi_\Lambda(x_1 - \xi)} < \frac{y_2}{y_1} \right\}} d\xi \pi(d\Lambda) \\
&= \frac{\beta}{\delta} (1 + \delta t) \int_{\mathbb{R}^d \times \mathcal{P}^d} \left[\frac{1}{y_1} \mathbf{1}_{\left\{ \frac{\varphi_\Lambda(z + \Delta_0)}{\varphi_\Lambda(z)} < \frac{y_2}{y_1} \right\}} - \frac{1}{y_2} \mathbf{1}_{\left\{ \frac{\varphi_\Lambda(z)}{\varphi_\Lambda(z - \Delta_0)} < \frac{y_2}{y_1} \right\}} \right] \varphi_\Lambda(z) dz \pi(d\Lambda).
\end{aligned}$$

Similarly, or by symmetry,

$$\begin{aligned}
\nu(B_2) &= \nu \left\{ \omega : \frac{y_1}{\varphi_\Lambda(x_1 - \xi)} \geq u > \frac{y_2}{\varphi_\Lambda(x_2 - \xi)}, \quad -\tau < \sigma \leq t \right\} \\
&= \frac{\beta}{\delta} (1 + \delta t) \int_{\mathbb{R}^d \times \mathcal{P}^d} \left[\frac{1}{y_2} \mathbf{1}_{\left\{ \frac{\varphi_\Lambda(z - \Delta_0)}{\varphi_\Lambda(z)} < \frac{y_1}{y_2} \right\}} - \frac{1}{y_1} \mathbf{1}_{\left\{ \frac{\varphi_\Lambda(z)}{\varphi_\Lambda(z + \Delta_0)} < \frac{y_1}{y_2} \right\}} \right] \varphi_\Lambda(z) dz \pi(d\Lambda).
\end{aligned}$$

For Gaussian kernels with $\varphi(z) \propto \exp(-z^2/2)$ more explicit expressions are available:

$$\begin{aligned}
\nu(B_0) &= \frac{\beta}{\delta} (1 + \delta t) \int_{\mathcal{P}^d} \left\{ \frac{1}{y_1} \Phi \left(\frac{1}{S_\Lambda} \log \frac{y_1}{y_2} - \frac{S_\Lambda}{2} \right) + \frac{1}{y_2} \Phi \left(\frac{1}{S_\Lambda} \log \frac{y_2}{y_1} - \frac{S_\Lambda}{2} \right) \right\} \pi(d\Lambda) \\
\nu(B_1) &= \frac{\beta}{\delta} (1 + \delta t) \int_{\mathcal{P}^d} \left\{ \frac{1}{y_1} \Phi \left(\frac{1}{S_\Lambda} \log \frac{y_2}{y_1} + \frac{S_\Lambda}{2} \right) - \frac{1}{y_2} \Phi \left(\frac{1}{S_\Lambda} \log \frac{y_2}{y_1} - \frac{S_\Lambda}{2} \right) \right\} \pi(d\Lambda) \\
\nu(B_2) &= \frac{\beta}{\delta} (1 + \delta t) \int_{\mathcal{P}^d} \left\{ \frac{1}{y_2} \Phi \left(\frac{1}{S_\Lambda} \log \frac{y_1}{y_2} + \frac{S_\Lambda}{2} \right) - \frac{1}{y_1} \Phi \left(\frac{1}{S_\Lambda} \log \frac{y_1}{y_2} - \frac{S_\Lambda}{2} \right) \right\} \pi(d\Lambda) \\
\nu(B_+) &= \frac{\beta}{\delta} (1 + \delta t) \int_{\mathcal{P}^d} \left\{ \frac{1}{y_1} \Phi \left(\frac{1}{S_\Lambda} \log \frac{y_2}{y_1} + \frac{S_\Lambda}{2} \right) + \frac{1}{y_2} \Phi \left(\frac{1}{S_\Lambda} \log \frac{y_1}{y_2} + \frac{S_\Lambda}{2} \right) \right\} \pi(d\Lambda)
\end{aligned}$$

where $S_\Lambda := \sqrt{(x_2 - x_1)' \Lambda (x_2 - x_1)}$ (this would be $S_\Lambda(0)$, for $v = 0$ in the notation introduced in the proof of Corollary 2.8).

For equal thresholds $y_1 = y_2 = y$, these have the simple form

$$\begin{aligned}
\nu(B_0) &= \frac{1}{y} \frac{\beta}{\delta} (1 + \delta t) \int_{\mathcal{P}^d} \{ 2\Phi(-S_\Lambda/2) \} \pi(d\Lambda) = \frac{1}{y} \frac{\beta}{\delta} (1 + \delta t) \quad (Z) \quad (\text{S.7}) \\
\nu(B_1) &= \nu(B_2) = \frac{1}{y} \frac{\beta}{\delta} (1 + \delta t) \int_{\mathcal{P}^d} \{ 2\Phi(S_\Lambda/2) - 1 \} \pi(d\Lambda) = \frac{1}{y} \frac{\beta}{\delta} (1 + \delta t) (1 - Z) \\
\nu(B_+) &= \frac{1}{y} \frac{\beta}{\delta} (1 + \delta t) \int_{\mathcal{P}^d} \{ 2\Phi(S_\Lambda/2) \} \pi(d\Lambda) = \frac{1}{y} \frac{\beta}{\delta} (1 + \delta t) (2 - Z)
\end{aligned}$$

for

$$Z := \int_{\mathcal{P}^d} 2\Phi(-S_\Lambda/2) \pi(d\Lambda). \quad (\text{S.8})$$

S4.3 Computing the distribution of $|\kappa_2 - \kappa_1|$

Set

$$\kappa_1 = \text{time until first exceedance of } y_1 \text{ at } x_1$$

- $\kappa_2 =$ time until first exceedance of y_2 at x_2
- $\kappa_1^* =$ time until first exceedance of y_1 at x_1 without exceeding y_2 at x_2
- $\kappa_2^* =$ time until first exceedance of y_2 at x_2 without exceeding y_1 at x_1
- $\kappa_0^* =$ time until first common exceedance,

Note that $\kappa_1 = (\kappa_0^* \wedge \kappa_1^*)$ and $\kappa_2 = (\kappa_0^* \wedge \kappa_2^*)$. Set

$$m_* := \min_{0 \leq j \leq 2} \kappa_j^*$$

for the minimum of $\{\kappa_j^*\}$, i.e., the time until the first exceedance.

Set $\lambda_j := \nu(B_j)/(1 + \delta t)$ for $j = 0, 1, 2$, so

$$\nu(B_j) = \lambda_j(1 + \delta t).$$

Then $\lambda_0 + \lambda_1 = \frac{\beta}{\delta y_1}$ and $\lambda_0 + \lambda_2 = \frac{\beta}{\delta y_2}$. In this notation, the distributions of κ_1 and κ_2 (given in (7)) and of m_* are given for $t \geq 0$ by

$$\mathbb{P}[\kappa_i > t] = e^{-(\lambda_0 + \lambda_j)(1 + \delta t)} \quad \mathbb{P}[m_* > t] = e^{-\lambda_+(1 + \delta t)},$$

each a mixture distribution with a point mass at zero and an exponential distribution. Next we consider the distribution of $|\kappa_2 - \kappa_1|$.

For $t \geq 0$, the event $|\kappa_2 - \kappa_1| > t$ can occur in four different ways, depending on which exceedance occurs first and whether or not the first occurs at time 0. First, the exceedances at time 0:

- $\kappa_1 = 0 < t < \kappa_2$:

$$\begin{aligned} \mathbb{P}[\kappa_1 = 0 < t < \kappa_2] &= \mathbb{P}[\kappa_1^* = 0 < t < (\kappa_0^* \wedge \kappa_2^*)] \\ &= (1 - e^{-\lambda_1})e^{-(\lambda_0 + \lambda_2)(1 + \delta t)} \end{aligned} \tag{S.9a}$$

- $\kappa_2 = 0 < t < \kappa_1$:

$$\begin{aligned} \mathbb{P}[\kappa_2 = 0 < t < \kappa_1] &= \mathbb{P}[\kappa_2^* = 0 < t < \kappa_0^* \wedge \kappa_1^*] \\ &= (1 - e^{-\lambda_2})e^{-(\lambda_0 + \lambda_1)(1 + \delta t)} \end{aligned} \tag{S.9b}$$

Next, those where the first exceedance $m_* > 0$ occurs after time zero, and the second after an additional time t .

- $0 < \kappa_1 < \kappa_1 + t < \kappa_2$:

$$\begin{aligned} \mathbb{P}[0 < \kappa_1 < \kappa_1 + t < \kappa_2] &= \mathbb{P}[(0 < m_*) \cap (\kappa_1^* = m_*) \cap (\kappa_2 > m_* + t)] \\ &= \mathbb{P}[m_* > 0] \mathbb{P}[\kappa_1^* = m_* \mid m_* > 0] \\ &\quad \times \mathbb{P}[(\kappa_0^* \wedge \kappa_2^*) > \kappa_1^* + t \mid (\kappa_0^* \wedge \kappa_2^*) > \kappa_1^* = m_* > 0] \\ &= \frac{\lambda_1}{\lambda_+} e^{-\lambda_+ - (\lambda_0 + \lambda_2)\delta t} \end{aligned}$$

- $0 < \kappa_2 < \kappa_2 + t < \kappa_1$:

$$\begin{aligned} \mathbb{P}[0 < \kappa_2 < \kappa_2 + t < \kappa_1] &= \mathbb{P}[(0 < m_*) \cap (\kappa_2^* = m_*) \cap (\kappa_1 > m_* + t)] \\ &= \frac{\lambda_2}{\lambda_+} e^{-\lambda_+ - (\lambda_0 + \lambda_1)\delta t} \end{aligned} \quad (\text{S.9c})$$

Summing the four cases, for $t \geq 0$ we have

$$\begin{aligned} \mathbb{P}[\kappa_\Delta > t] &= e^{-(\lambda_0 + \lambda_2)(1 + \delta t)} \left[1 - \frac{\lambda_0 + \lambda_2}{\lambda_+} e^{-\lambda_1} \right] \\ &\quad + e^{-(\lambda_0 + \lambda_1)(1 + \delta t)} \left[1 - \frac{\lambda_0 + \lambda_1}{\lambda_+} e^{-\lambda_2} \right], \end{aligned} \quad (\text{S.10})$$

a mixture of two exponential distributions and a point mass at zero of mass

$$\mathbb{P}[\kappa_\Delta = 0] = 1 - e^{-\lambda_0} (e^{-\lambda_1} + e^{-\lambda_2}) + e^{-\lambda_+} \left(1 + \frac{\lambda_0}{\lambda_+} \right).$$

S5 Gibbs sampler for mixture models

Consider the Bayesian model

$$\kappa \sim q_0 \delta_0 + \sum_{j=1}^{K-1} q_j \text{Exponential}(\lambda_j) \quad (\text{S.11})$$

$$q \sim \text{Dirichlet}(\boldsymbol{\alpha}), \quad \lambda_j \stackrel{iid}{\sim} \text{Gamma}(a, b). \quad (\text{S.12})$$

For observed waiting times κ_i for $i \in \{1, \dots, N\}$, a Gibbs sampler for this model, including imputation of continuous waiting times from censored waiting times, cycles through the following steps

1. For each observation $i \in \{1, \dots, N\}$, sample a latent variable $z_i \sim \text{Categorical}(\tilde{q})$, where

$$\tilde{q}_j = \begin{cases} \frac{q_j \lambda_j e^{-\lambda_j \tilde{\kappa}_i}}{q_0 \mathbf{1}_{\{\tilde{\kappa}_i = 0\}} + \sum_{j=1}^K \lambda_j e^{-\lambda_j \tilde{\kappa}_i}} & j > 0 \\ \frac{q_0 \mathbf{1}_{\{\tilde{\kappa}_i = 0\}}}{q_0 \mathbf{1}_{\{\tilde{\kappa}_i = 0\}} + \sum_{j=1}^K \lambda_j e^{-\lambda_j \tilde{\kappa}_i}} & j = 0 \end{cases}$$

2. Sample λ_j from

$$\lambda_j \sim \text{Gamma} \left(a + \sum_i \mathbf{1}_{\{z_i = j\}}, b + \sum_i \tilde{\kappa}_i \mathbf{1}_{\{z_i = j\}} \right).$$

3. Sample q from

$$q \sim \text{Dirichlet} \left(\alpha + \sum_i \mathbf{1}_{\{z_i = 1\}}, \dots, \alpha + \sum_i \mathbf{1}_{\{z_i = K\}} \right)$$

4. Sample $w_i \sim \text{Categorical}(\tilde{q})$ where

$$\tilde{q}_j = \begin{cases} \frac{q_j (F_{\lambda_j}(\kappa_i+1) - F_{\lambda_j}(\kappa_i))}{q_0 \mathbf{1}_{\{\kappa_i=0\}} + \sum_j q_j (F_{\lambda_j}(\kappa_i+1) - F_{\lambda_j}(\kappa_i))} & j > 0 \\ \frac{q_0 \mathbf{1}_{\{\kappa_i=0\}}}{q_0 \mathbf{1}_{\{\kappa_i=0\}} + \sum_j q_j (F_{\lambda_j}(\kappa_i+1) - F_{\lambda_j}(\kappa_i))} & j = 0 \end{cases}$$

then sample

$$\tilde{\kappa}_i \sim \begin{cases} \delta_0 & w_i = 1 \\ \text{Exponential}_{[\kappa_i, \kappa_i+1]}(\lambda_j) & w_i = j + 1 \end{cases}$$

where $\text{Exponential}_{[l,u]}$ is an exponential distribution truncated to the interval $[l, u]$.

S6 Supplemental Figures

Table S1: Key indicating identity of currencies in Figure 6.

col./row #	symbol	name	col./row #	symbol	name
1	AUD	Australian Dollar	7	NLG	Dutch Guilder
2	BEF	Belgian Franc	8	NZD	New Zealand Dollar
3	CAD	Canadian Dollar	9	ESP	Spanish Peseta
4	FRF	French Franc	10	SEK	Swedish Kroner
5	DEM	German Deutschmark	11	CHF	Swiss Franc
6	JPY	Japanese Yen	12	GBP	British Pound

Table S2: Key indicating identity of stocks in the images in Figure 5

col./row #	symbol	name	col./row #	symbol	name
1	axp	American Express	16	mcd	McDonald's
2	ba	Boeing	17	mmm	3M
3	cat	Caterpillar	18	mrk	Merck
4	csc	Cisco Systems	19	msft	Microsoft
5	cvx	Chevron	20	nke	Nike
6	dd	DuPont	21	pfe	Pfizer
7	dis	Disney	22	pg	Proctor & Gamble
8	ge	General Electric	23	t	AT&T
9	gs	Goldman Sachs	24	trv	Travelers
10	hd	Home Depot	25	unh	United Healthcare
11	ibm	IBM	26	utx	United Technologies
12	intc	Intel	27	v	Visa
13	jnj	Johnson & Johnson	28	vz	Verizon
14	jpm	J.P. Morgan Chase	29	wmt	Wal-Mart
15	ko	Coca-Cola	30	xom	Exxon-Mobil

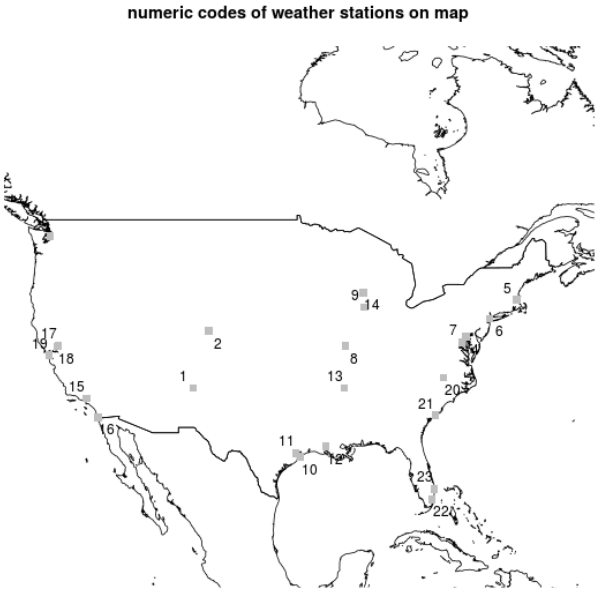


Figure S1: Map with numbers labeling locations of weather stations; the numbers correspond to the order in which the stations appear in the colormap images in Figure 4.

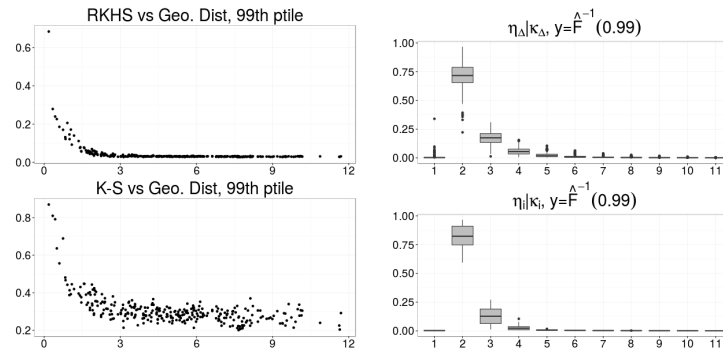


Figure S2: Left: plots of $\hat{\gamma}_d$ for $d = W_{1,\varphi}$ and $d = TV$ for threshold $y_i = \hat{F}_i^{-1}(0.99)$ versus Euclidean distance between points. Right: Posterior estimates of $\eta_i | \kappa_i$ and $\eta_{\Delta} | \kappa_{\Delta}$ for $y = F^{-1}(0.99)$.